iScience

CellPress
OPEN ACCESS

Review

Nanoarchitecting Hierarchical Mesoporous Siliceous Frameworks: A New Way Forward

Ranjith Kumar Kankala,[1,2,3,*] Shi-Bin Wang,[1,2,3] and Ai-Zheng Chen[1,2,3,*]

SUMMARY

Owing to their attractive physicochemical and morphological attributes, mesoporous silica nanoparticles (MSNs) have attracted increasing attention over the past two decades for their utilization in diversified fields. Despite the success, these highly stable siliceous frameworks often suffer from several shortcomings of compatibility issues, uncontrollable degradability leading to long-term retention *in vivo*, and substantial unpredictable toxicity risks, as well as deprived drug encapsulation efficiency, which could limit their applicability in medicine. Along this line, various advancements have been made in re-engineering the stable siliceous frameworks, such as the incorporation of diverse molecular organic, as well as inorganic (cationic and anionic) species and monitoring the processing, as well as formulation parameters, resulting in the hetero-nanostructures of irregular-shaped (Janus and multi-podal) and dynamically-modulated (deformable solids) architectures with high morphological complexity. Insightfully, this review gives a brief emphasis on re-engineering such stable siliceous frameworks through modifying their intrinsic structural and physicochemical attributes. In conclusion, we recapitulate the review with exciting perspectives.

INTRODUCTION

Indeed, the rapid progress in the field of nanotechnology has evidenced the fabrication of various smart materials with exceptional performance, providing enormous opportunities in diversified fields of science and technology (Riehemann et al., 2009). Owing to their abundant surface chemistry and high surface-to-volume ratio, the nano-sized materials (1–100 nm in one or more dimensions) offer size-, as well as shape-dependent tunable morphological and physicochemical attributes, including mechanical, magnetic, optical, and electronic properties, which are of particular importance in various fields (Mekaru et al., 2015; Xia, 2008). In addition, several other attributes of some of the nanomaterials include ease of scalability and cost-effectiveness. As a result, tremendous interest from researchers in the use of such pioneering materials continued to rise (Chen et al., 2013; Liong et al., 2008; Niu et al., 2011). Among various inorganic material-based porous nanoconstructs, mesoporous silica nanoparticles (MSNs) have attracted enormous interest due to their advantageous physicochemical attributes, as well as tunable morphological features, such as extensive surface area and pore volume, unique topology (surface and inner porous architectures), adjustable uniform-sized mesopores, as well as tunable particle sizes and shapes, in many highly ordered and complex structures (Kankala et al., 2019; Slowing et al., 2008). The properties of exceptional topology and abundant surface chemistry enable them to be unique with desirable properties that facilitate the ease of surface functionalization (both interior and exterior) and contribute to the colloidal stability, as well as high dispersity of the surfactant-templated MSNs. Such properties of MSNs can be altered by well regulating the synthesis conditions (Hu et al., 2011; Wu et al., 2013). It should be noted that the aforementioned advantages of MSNs, along with low cost and ease of synthesis, facilitated their utilization towards widespread applicability in different fields including but not limited to adsorption, catalysis, gas sensing, metal extraction, optical devices, lithium storage, as well as fabrication of metal oxides, and medicine, among others (Kankala et al., 2020a; Lee et al., 2009; Lin et al., 2005).

Since ever the first report of the well-ordered crystalline molecular sieves, named Mobil Composition of Matter (MCM)-41 in the early 1990s (Beck et al., 1992; Kresge et al., 1992), several efforts have been dedicated to successfully fabricating various advanced prototypes of the MCM family, such as MCM-48 and MCM-50 with cubic and lamellar mesophases, respectively (Wu et al., 2013). Briefly, these well-ordered crystalline molecular sieves are constructed by depositing the silica precursor over the amphiphilic surfactant

[1]College of Chemical Engineering, Huaqiao University, Xiamen, Fujian 361021, P. R. China

[2]Institute of Biomaterials and Tissue Engineering, Huaqiao University, Xiamen, Fujian 361021, P. R. China

[3]Fujian Provincial Key Laboratory of Biochemical Technology (Huaqiao University), Xiamen, Fujian 361021, P. R. China

*Correspondence: ranjithkankala@hqu.edu.cn (R.K.K.), azchen@hqu.edu.cn (A.-Z.C.)

https://doi.org/10.1016/j.isci.2020.101687

molecules, resulting in the formation of uniform-sized mesopores (1.5-10 nm) (Lee et al., 2009; Yang et al., 2019). Notably, such confined frameworks of MCM-41 in the nano-size range were used for delivering ibuprofen, which resulted in sustained release behavior in the aqueous microenvironment. Motivated by these facts, MSNs were then popularized in the early and mid 2000s by Grun, Mou, Lin, Cai, Shi, and Mann, among others, in fabricating small-sized MSNs (30-100 nm) by stringently monitoring the critical synthesis conditions (pH value and temperature of the reaction medium, stirring speed, and type of silica source, as well as the surfactant, among others) (Cai et al., 2001; Chen et al., 2013; Fowler et al., 2001; Grün et al., 1997; He et al., 2010; Lai et al., 2003). Owing to their various structures, dimensions, morphologies, and pore sizes, MSNs offer several advantages of abundant surface chemistry for the functionalization of mesoporous surface and appropriate biocompatibility, as well as colloidal stability in the physiological environment (Kankala et al., 2020c). These advancements significantly motivated the researchers in using MSNs as promising drug delivery vehicles toward fabricating advanced stimuli (light, magnetic, molecular, pH, and thermos, among others)-responsive and active targeted systems to alter their pharmacokinetic behavior, as well as biocompatibility and toxicity attributes, for better theranostic efficiency (Chen et al., 2013; Rosenholm et al., 2009, 2010).

Bothering Intrinsic Limitations

Despite the advantageous tunable morphological and physicochemical attributes, these highly stable mesoporous siliceous frameworks are merely supported as vectors for conveying various therapeutic guest species and imaging agents, which are of particular interest in diverse biomedical applications (Kankala et al., 2019; Rosenholm et al., 2016). Although MSNs offer excellent carrying ability due to their high specific surface area, these siliceous frameworks suffer from various shortcomings, such as reduced drug encapsulation and delivery efficiencies, degradability, as well as compatibility concerns to a considerable extent, which significantly limit their utility in medicine. More often, the encapsulation efficiency of guest species in the pores of MSNs is predominantly dependent on their affinities with the MSN host, which are managed by the weak interactions within the mesopores. Further, these weak interactions could lead to the rapid release of the encapsulated guest species or subsequent exchange with the surrounding ionic species not only during their encapsulation but also during delivery processes, leading to reduced encapsulation and delivery efficiencies of therapeutic cargo (Kankala et al., 2017; Liu et al., 2019; Slowing et al., 2008).

Furthermore, the predominant attribute that influences the applicability of naked MSNs is the poor degradability of such stable siliceous frameworks, as the conventional hydrothermal-assisted synthetic process of MSNs often results in highly stable, inert, and robust siliceous frameworks (Croissant et al., 2014a). Due to their rigid siloxane (-Si-O-Si-) network, these MSNs with highly ordered structures are relatively more stable compared to those of polymers and other inorganic porous carriers (Croissant et al., 2014a; Huang et al., 2017; Wang et al., 2017). However, there exist some reports that these rigid siloxane species could offer a certain degree of degradation by slow hydrolysis, resulting in corresponding silanol groups (-Si-OH) in the aqueous environment. It should be noted that this partial degradation is dependent on various factors that regulate the hydrolysis process, such as the degree of siliceous framework condensation, presence of organic or inorganic chemical functionalities, overall specific surface area, eventual particle size, and porosity (Croissant et al., 2014a; Kankala et al., 2020a; Shen et al., 2014). Noteworthy, the degree of siliceous frameworks degradation is progressively decelerated owing to the presence of various ions, such as calcium and magnesium, in the physiological fluids, resulting in the formation of a stable metal silicate layer, which, however, degrades completely at a permissible low concentration (Chen et al., 2013; Wang et al., 2017). Conclusively, the partial degradation ability due to the hydrolysis of MSNs indicates the uncontrollable nature of the degradation behavior of MSNs. To this end, there exist specific reports of the fabrication of ultrasmall-sized silicon dots (<10 nm) and porous silicon-based materials that boosted the utilization of silica (Du et al., 2018a). In addition, several studies on polymer-coated MSNs, for instance, polyethylene glycol coating (PEGylation) and others, with partial or reduced degradation ability, have been reported. However, lack of sufficient tools to monitor this property is another challenge that is faced in the translation of MSNs (Dinker and Kulkarni, 2016; He et al., 2010). In addition, contrary findings in the literature in terms of particle size of MSNs emphasize that the small-sized particles could retain longer in the blood circulation with slower degradation rates, while the particles with the average diameter of >100 nm would get excreted rapidly through hepatic and renal excretion routes in the form of partially degraded products (He et al., 2011). The mechanistic insights lying behind the elimination of MSNs from the body yet remained to be explored.

Notably, the cellular internalization efficiency of bare MSNs is limited due to their negatively charged frameworks, which could be repelled by the negatively charged biological membranes. Although

overcoming the extracellular repulsions by modifying the surface of MSNs with the contrary charged biopolymers, the intracellular interactions with the organelles would be highly challenging. Considering this aspect, re-engineering the siliceous frameworks toward altering the net surface charge has created the enormous possibility for addressing such intrinsic limitations of MSNs. Incorporating the first-row-transition metal species is one of the appropriate choices for overcoming this issue. In addition, the siliceous frameworks can be engineered by incorporating the flexible moieties that facilitate the change in shape, such as deformability, for the ease of cellular internalization of MSNs (Teng et al., 2018). Moreover, it is also feasible to immobilize the cell-penetrating peptides (for instance, poly (disulfide)s and a fluorogenic apoptosis-detecting peptide, Asp-Glu-Val-Asp-2-acetyl-6-amino naphthalene, DEVD-AAN) or organelle-targeting moieties over the MSN surface, such as nuclear localization signal, and mitochondrial targeting sequence, transactivator of transcription (TAT, GRKKRRQRRRPQ) peptides (Jhaveri and Torchilin, 2016; Liu et al., 2020; Yu et al., 2016). These modifications may facilitate not only overcoming the endolysosomal trapping but also subsequently achieving the organelle-targeted delivery of the therapeutic cargo towards better therapeutic efficacy.

Indeed, MSNs are known for their biocompatibility as the siliceous frameworks result in the non-toxic silicic acid species in the physiological fluids. Despite the presence of such highly functional surface hydroxyl groups that do not influence some of the cell lines *in vitro*, however, in some of the instances, these stable siliceous frameworks exhibit toxicity signs (Hudson et al., 2008). Although there have been several advancements in engineering the structure of MSNs such as periodic mesoporous organosilicas (PMOs), as well as disulfide-bridged composites and other derivatives of deformable architectures, toward addressing the compatibility and degradability issues (Abbaraju et al., 2017; Croissant et al., 2014a; Du et al., 2018a; Liu et al., 2019; Yamada et al., 2012; Yang et al., 2016b; Zhou et al., 2017), however, the biosafety of MSNs and their fate *in vivo* remained as serious complications, which are substantially hampering their progression towards clinical translation (Williams, 2008). Moreover, the viewpoint and detailed mechanistic insights of the biosafety of MSNs *in vivo* remained unclear due to the complex biological environment with numerous tissue barriers and lack of real-time high-resolution bioimaging strategies (Chen et al., 2013). Along this line, numerous reports demonstrated the compatibility attributes of MSNs in various levels ranging from cellular *in vitro* to animal studies *in vivo* by multiple modifications (Kankala et al., 2019, 2020a). In the vein of enhancing their physicochemical characteristics, multiple advancements have been made, such as surface coating of biocompatible polymers/peptides/biological membranes (Niedermayer et al., 2015; Shao et al., 2018; Zhang et al., 2015b), tethering the responsive linkers enabling their degradation (Croissant et al., 2014a; Du et al., 2018a; Maggini et al., 2016; Wang et al., 2019c), and modifying the siliceous frameworks (Kankala et al., 2015; Liu et al., 2019), as well as mesopore ordering (Niu et al., 2010; Wang et al., 2016), among others. Such innovative modifications enable tuning the sizes, surfaces, and siliceous frameworks toward fabricating the sophisticated, complex architectures by innovative chemistries (Wen et al., 2017).

Despite numerous reports and review articles on MSNs and their successive hybrid composites by other groups and us have been published so far (Argyo et al., 2014; Chen et al., 2013; Croissant et al., 2014a, 2015b, 2018; Du et al., 2018a; Kankala et al., 2019, 2020a; Lee et al., 2009, 2011; Maggini et al., 2016; Mekaru et al., 2015; Popat et al., 2011; Rosenholm et al., 2010, 2016; Slowing et al., 2008; Tao, 2014; Tarn et al., 2013; Teng et al., 2019; Trewyn et al., 2007; Wang et al., 2015; Wen et al., 2017; Wu et al., 2011, 2013; Yanes and Tamanoi, 2012; Yang et al., 2019), the scope of the review emphasizes the significant progress in the field of MSNs, specifically highlighting the engineered mesoporous siliceous frameworks. To the best of our knowledge, although enormous efforts have been made in reviewing or summarizing the MSNs, notably, all the articles have confined the discussions on their subtypes or by focusing on the specific applications. However, in this article, we emphasize the modifications of the highly stable mesoporous siliceous frameworks using diverse organic and inorganic molecular assemblies and interdependent relationships toward the utilization of these hybrids in diverse applications. Initially, we provide an overview of the critical advancements made in modifying the mesoporous siliceous frameworks in the past few years by other groups and us toward addressing the intrinsic limitations of MSNs. In addition, we emphasize the scope of advancements of these modified MSNs toward diverse applications by modifying their inherent structural and physicochemical attributes. Various critical advancements, such as impregnation of diverse molecular organic, as well as inorganic (cationic and anionic) assemblies and monitoring the processing, as well as formulation parameters, resulting in the hetero-nanostructures of irregular-shaped (Janus and multi-podal) and dynamically-modulated (deformable solids) architectures with high morphological complexity, are discussed (Figure 1). Notably, these re-engineered complex architectures substantially promise to offer exceptional performance along with inherent stability, stimuli (pH/light/molecular)-responsive release,

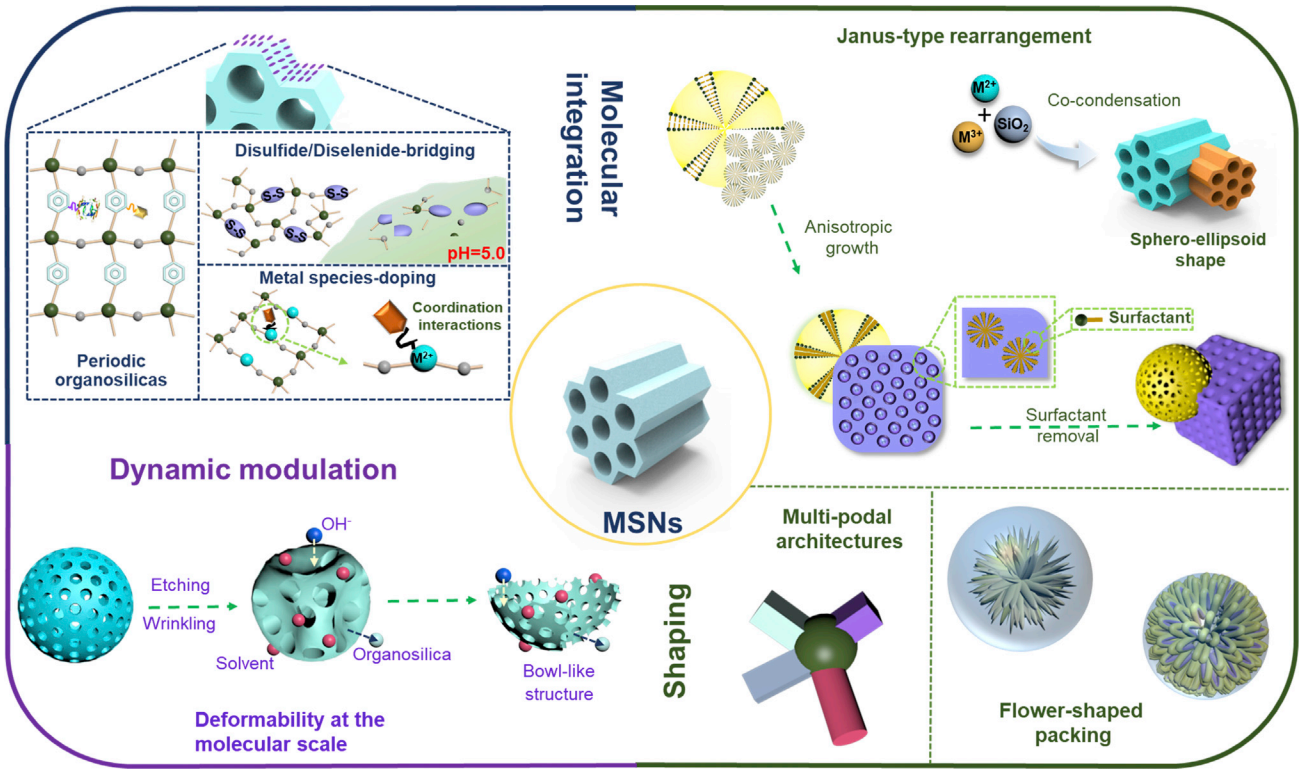

Figure 1. Schematic Illustrating the Re-engineering of the Highly Rigid, Hierarchical Siliceous Frameworks toward the Fabrication of Diversified Molecular-Integrated, Dynamically-Modulated, and Asymmetrical-Shaped Architectures.

degradation, as well as compatibility tendencies *in vivo*. Finally, we recapitulate the review with intriguing perspectives and outlook toward their translation from research to scale-up.

FABRICATION OF MSNS

Indeed, the mesoporous siliceous frameworks are often fabricated using the conventional templating approach. In this context, the formation of MSNs is predominantly based on the assembly of surfactant and silica species during the co-condensation, as well as specific electrostatic interactions involved between the components of the organic structure-directing surfactant template, typically cetyl trimethyl ammonium bromide (CTAB), and condensed silica (Argyo et al., 2014; Wu et al., 2013). Moreover, it is dependent on not only the thermodynamics behind the assembly of surfactant molecules in their critical micelle concentration and silica species but also the controlled reaction kinetics, resulting in the diversified morphologies and dimensions of the resultant siliceous matrices through establishing the electrostatic interactions between them (Argyo et al., 2014; Wu et al., 2013). In addition to the control over the self-assembly and silica condensation rate, it is highly convenient to fabricate various mesostructured architectures, ranging from disordered assemblies to ordered lamellar mesophase-based structures due to their liquid crystalline mesophases and altered morphological attributes in the assembly of surfactants. Accordingly, nano-sized silica composites in the range of tens to hundreds of nanometers with mesoporous architectures and uniform morphological attributes have been successfully reported (Argyo et al., 2014; Cai et al., 2001; Fowler et al., 2001; Grün et al., 1997; Huh et al., 2003; Suteewong et al., 2013; Wu et al., 2013).

Notably, various factors significantly influence the fabrication of such siliceous frameworks during the traditional co-condensation process. Along this line, two variables, *i.e.,* formulation and processing factors, significantly play crucial roles in the final size distribution and mesoporosity of MSNs. Among the formulation factors, the selection of an appropriate concentration of the cationic surfactant plays a crucial role in generating MSNs with ordered lamellar mesophases in the appropriate size range. Further, enormous efforts have been dedicated to fabricating hollow MSNs (HMSNs) and their respective nanorods, as well as many other types with diverse morphologies by utilizing various soft and hard templating approaches

(polymers, fluorocarbons, Pluronic block, polystyrene-b-poly (acrylic acid), PS-b-PAA copolymers, as well as diverse metal species, respectively) (Chen et al., 2014; Geng et al., 2017; Li et al., 2017; Lou et al., 2008; Teng et al., 2019; Wang et al., 2020; Wu et al., 2013; Zhang et al., 2015a). Concerning the processing parameters, the pH value of the reaction medium plays a predominant role as it significantly influences the eventual charge of the silica species, affecting the hydrolysis and subsequent co-condensation of silica species. Although the synthesis is favorable in alkaline, acidic, and neutral pH conditions, based on the isoelectric point (IEP) value, the charge of silica varies in different pH values of the synthesis solution, such that the negative charge at a pH above to its IEP and *vice versa* (Wu et al., 2013). Nevertheless, the silicates with high charge densities are assembled at the alkaline conditions, yielding small-sized nanocontainers with even particle size distribution. In addition, at the moderate temperature and mildly acidic conditions, it is convenient to fabricate hierarchical mesoporous silica networks and their prototypes, Institute of Bioengineering and Nanotechnology (IBN)-series architectures with tunable 2D hexagonal, 3D cubic, disordered, and foam-like pore structures (Han and Ying, 2005; Wang, 2010). It should be noted that the rate of silica hydrolysis is faster in alkaline conditions over the acidic solutions. Although the extreme pH conditions are favorable, the neutral environment also favors the formation of MSNs with the highest rate constant of self-condensation (Wu et al., 2013). The solvent in the reaction medium that provides alkalinity facilitates the rapid precipitation of silica over the surfactant template. The most commonly used solvent in the modified Stober approach is ammonia. In addition, sodium hydroxide is used as a solvent, referring to the pseudomorphic synthesis that can be applied for the transformation processes. Moreover, other solvents such as triethanolamine can also be used to fabricate ultrasmall-sized MSNs (~20 nm), which offer exceptional colloidal stability and high suitability toward diverse biomedical applications (Huh et al., 2003). Consequently, the remarkable attentiveness from researchers in utilizing such ground-breaking materials through conveniently altering the formulation and fabrication parameters continues to increase.

ENGINEERING MESOPOROUS SILICEOUS FRAMEWORKS

Since ever the inception, the scope of advancements towards addressing certain aforementioned limitations of MSNs has garnered enormous attention from researchers, which, however, confined to three crucial aspects (Kankala et al., 2020a). First, owing to the high density of surface hydroxyl groups on MSNs, the hydrophilic surface can be conveniently modified through chemical functionalization and immobilization of targeting ligands for precisely directing them to the desired target sites (Liong et al., 2008; Mekaru et al., 2015). Second, the controllable porosity of these highly ordered architectures can be restructured using swelling agents or enhancers during the chemical synthesis, which can substantially accommodate large-sized or highly dense guest species. Third, more importantly, the modifications in the stable patterns of siliceous frameworks can be achieved by various modifications such as incorporating various molecular organic and inorganic (cationic and anionic) assemblies, as well as altering the processing and formulation parameters, among others. Figure 2 illustrates the timeline progress of breakthroughs in tuning the mesoporous siliceous frameworks since the fabrication of 3D molecular sieves to recent advancements in terms of framework modifications. Such re-engineered highly complex architectures also result in the hetero-nanostructures of irregular-shaped (Janus, and multi-podal) and dynamically-modulated (deformable solids) architectures with high morphological complexity toward promising exceptional performance along with inherent stability, stimuli (pH/molecular)-responsive release, biodegradation, and compatibility *in vivo* (Figures 1 and 2, Table 1). Moreover, these modifications often result in substantial changes in the overall morphology (particle sizes and shaping), as well as other physicochemical properties such as suspension ability, various stability attributes, and surface characteristics, which are of specific interest in different biomedical applications, including bioimaging, drug delivery, and tissue engineering, among others (Kankala et al., 2015, 2019; Landau et al., 2001; Lee et al., 2009; Slowing et al., 2008). Notably, these advancements have facilitated MSNs toward becoming one of the essential classes of porous materials for their application in diversified fields of science (Liong et al., 2008).

Concerning the field of medicine, although various modifications such as engineering the surface and mesopore have addressed most of the aforementioned limitations, the precise engineering of the siliceous frameworks can specifically overcome certain intrinsic limitations of MSNs that are highly challenging with the other two kinds of modifications. Notably, the degradability of siliceous frameworks in the physiological environments is an essential attribute, which is one way or another related to the biocompatibility of these emerging species. Owing to the inherent stability that leads to poor degradability and other biocompatibility issues, the applicability *in vivo* and subsequent clinical translation of these inorganic porous architectures are significantly hindered, as the difficulties of elimination from the body through combating hierarchical bio-barriers remained to be addressed comprehensively (Chen et al., 2013;

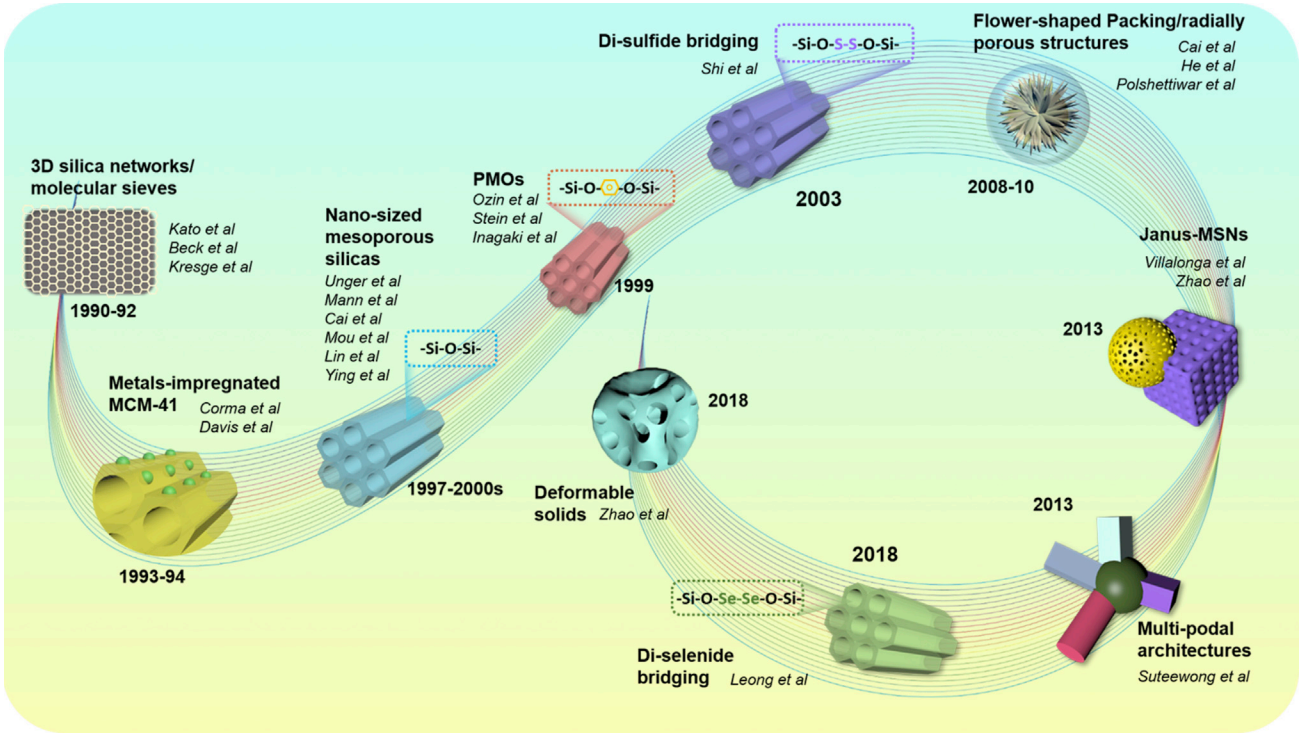

Figure 2. Schematic Illustrating the Timeline Progress of Breakthroughs in Tuning or Nanoarchitecting the Mesoporous Siliceous Frameworks.

Croissant et al., 2014a; Du et al., 2018a; Kankala et al., 2019). In addition, the encapsulation efficiency of various guest species in mesopores can be significantly improved by impregnating various organic or inorganic moieties in these stable frameworks, which not only enhance the loading through establishing coordination interactions with them but also facilitate stimuli-responsive release (Du et al., 2016; Kankala et al., 2020c). To a considerable extent, these issues could be addressed through applying various ways of altering the arrangement patterns of siloxane species, such as integrating organic molecules (PMOs), disulfide/diselenide bridging, and various metal (divalent and trivalent) species (Croissant et al., 2014a; Du et al., 2016; Kankala et al., 2020c). In addition, various advancements by reshuffling the molecular arrangement patterns have been made to redesigning such architectures toward Janus-type architectures and nature-mimicking designs, for instance, flower-shaped assemblies (Li et al., 2014; Xu et al., 2015; Xuan et al., 2016). Moreover, other specific classes of engineered siliceous frameworks such as multi-podal siliceous architectures and highly deformable solids are also designed for expanding the applicability of MSNs in medicine (Teng et al., 2018). In the further sections, critical facts on various aspects of tuning the MSN frameworks are comprehensively explored, highlighting the pros and cons, as well as mechanisms and scope involved for their applicability towards the landscape of clinical translation.

Molecular Integration

Incorporating diverse molecular assemblies in the mesoporous siliceous pool is indeed a distinctive approach for garnering multiple functionalities of the discrete components, facilitating the innovative possibilities toward diverse applications (Croissant et al., 2014a; Wen et al., 2017). By providing unique optical, electronic, and physicochemical attributes, various integrated molecular species, such as organic and inorganic cations, as well as anions (disulfide/diselenide), and supramolecular moieties, act as stimuli (pH/light/molecular/thermos)-triggering switches. Such impregnated constructs facilitate enormous advantages toward delivering diverse therapeutic guest species and addressing the intrinsic limitations by improving the degradability and compatibility attributes toward their applicability in medicine (Chen et al., 2011a).

PMOs

PMOs are often referred to as a homogeneous fusion of various organic moieties, for instance, organo-bridged silanes, with the inorganic siliceous architectures through covalently bonded unique composite

Type of Tuning		Precursors	Particle Size (nm)	Outcome/Benefits	References
Molecular integration	Periodic mesoporous organosilicas (PMOs)	Benzene, ethylene, ethane, 2,2′-bipyridine, thiophene, divinylbenzene, biphenyl, bis-imidazolium, among others	20–500 nm	These organo-inorganic hybrid composites offer improved compatibility, degradability, and chemical, electronic, mechanical, magnetic, as well as optical properties.	(Asefa et al., 1999; Cho et al., 2009; Croissant et al., 2014a, 2014b, 2016a; Dinker and Kulkarni, 2016; Du et al., 2016; Grosch et al., 2015; Inagaki et al., 1999; Maegawa and Inagaki, 2015; Sayari and Wang, 2005)
	Disulfide-bridged constructs	Bis (triethoxysilyl propyl) disulfide, (- $(CH_2)_3$-S ~ S-$(CH_2)_3$-)	20–350	Enhanced GSH-triggered biodegradation through a disulfide-thiol exchange reaction.	(Croissant et al., 2014a; Du et al., 2018b; Kim et al., 2012; Quesada et al., 2013; Teng et al., 2014; Zhang et al., 2003; Zhou et al., 2017)
		Bis (triethoxysilyl propyl) tetrasulfide (- $(CH_2)_3$-S ~ S ~ S ~ S- $(CH_2)_3$-)	30–2000	-do-	(Wu et al., 2015; Yang et al., 2016b)
	Diselenide-bridged constructs	Se-Se	~50 nm	Rapid GSH-triggered biodegradation over the disulfide linkage due to weaker electronegativity.	(Shao et al., 2018)
	Metal-impregnated mesoporous silicas	Al	–	Incorporated Al species (Al-MCM-41/Al-MCM-48) enhanced the acidity for catalysis applications.	(Aspromonte et al., 2012; Cesteros and Haller, 2001; Chen et al., 1993; Corma et al., 1994; Eimer et al., 2002; Huo et al., 2014; Kolodziejski et al., 1993; Monnier et al., 1993; Ryoo et al., 1997)
		Cu	~100	Offered pH-responsive release and degradation of MSNs.	(Kankala et al., 2015, 2017, 2020b; Kuthati et al., 2017; Liu et al., 2019)
		Fe	50–150	Facilitated the unique chemical coordination-accelerated biodegradation.	(Wang et al., 2017)
		Co, Fe, Ni	–	Influenced the adsorption capacity, activity, and stability of the catalysts.	(Parvulescu and Su, 2001)
		Zn	~100	Offered pH-responsive release of therapeutic guests in MSNs.	(Kankala et al., 2020a, 2020c)

Table 1. Examples of Various Nanoarchitecting Approaches toward Tuning the Stable Siliceous Frameworks

(Continued on next page)

Type of Tuning		Precursors	Particle Size (nm)	Outcome/Benefits	References
Shaping	Janus-type architectures	Gold, platinum, upconverting nanoparticles (UCNPs), iron oxide, and first-row-transition metal species	30–300	Metal-associated asymmetric shaped constructs with well-defined particle sizes showed improved magnetic, electrical, and optical, as well as mobility characteristics.	(Abbaraju et al., 2017; Karimi et al., 2017; Li et al., 2014; Liu et al., 2019; Ma et al., 2015; Shao et al., 2016; Ujiie et al., 2015; Villalonga et al., 2013; Wang et al., 2019c; Xuan et al., 2016)
	Multi-podal/multi-compartment architectures	Ethyl acetate, mixed organosilane precursors	100–200	Multi-compartment nanocontainers offered selective drug adsorption for multidrug delivery.	(Croissant et al., 2015a; Suteewong et al., 2013; Zhao et al., 2019)
	Flower-shaped packing/ dendritic/radially porous designs	Adding cosolvents (diethyl ether, pentanol) and utilizing catalysts (triethanolamine, reduced ammonia), 4-mercaptophenylacetic acid, poly (acrylic acid), and altered emulsion components ratio	50–200	Center-wide radial porous channels offered improved encapsulation of large-sized therapeutic molecules.	(Das et al., 2019; Du and Qiao, 2015; Gao et al., 2017; Wang et al., 2013, 2019a, 2019b; Xu et al., 2015; Zheng et al., 2018)
Dynamic modulation	Deformable solids	PMO (thioether/benzene/ethane-bridged)-based siliceous shells	50–200	Enriched the cellular internalization by changing their overall morphology (spherical-to-oval) during the mechanical inner stress.	(Teng et al., 2018)

Table 1. Continued

networks. Such hybrid structures offer improved intrinsic functionalities and morphological attributes of nano-sized mesoporous silicas owing to their higher organic content, *i.e.*, greater than 2-fold compared to organically-doped silicas (Figure 3A) (Asefa et al., 1999; Croissant et al., 2016a; Du et al., 2016; Inagaki et al., 1999; Melde et al., 1999). These hybridized organic-inorganic architectures substantially result in altered surface chemistry compared to pristine MSNs and organosilicas, which is of particular interest towards various applications, such as adsorption, catalysis, drug delivery, enzyme immobilization, protein separation, and as templates in the synthesis of nano-sized frameworks (Croissant et al., 2015b; Du et al., 2018a; Fang et al., 2018; Teng et al., 2018; Tian et al., 2017). Since ever the investigations of traditional MSNs toward biomedical applications were underway, parallel efforts by Inagaki, Stein, and Ozin, in the year 1999, were dedicated to incorporating the facile organo-silane precursors comprising of benzene, ethylene, and ethane, as bridging groups in the channel walls (Asefa et al., 1999; Inagaki et al., 1999; Melde et al., 1999). Notably, the generation of such PMOs was predominantly focused on enhancing the utility of MSNs with improved chemical, electronic, magnetic, mechanical, and optical properties (Asefa et al., 1999). Further efforts have been dedicated to fabricating PMOs with different morphological attributes (in the arbitrary size range of 20–500 nm) using various precursors, such as 2,2′-bipyridine (Maegawa and Inagaki, 2015), thiophene (Cho et al., 2009), divinylbenzene (Sayari and Wang, 2005), biphenyl (Grosch et al., 2015), and bis-imidazolium (Dinker and Kulkarni, 2016), among others (Du et al., 2016; Waki et al., 2014). However, the applicability of PMOs could be significantly attributed to the hydrophobicity/hydrophilicity of the silsesquioxane moieties in the mesoporous frameworks (Du et al., 2016).

In addition to providing improved physicochemical properties, these PMOs offer enormous advantages in terms of their utility over the traditional MSNs. Concerning the biomedical applications, the increase in the

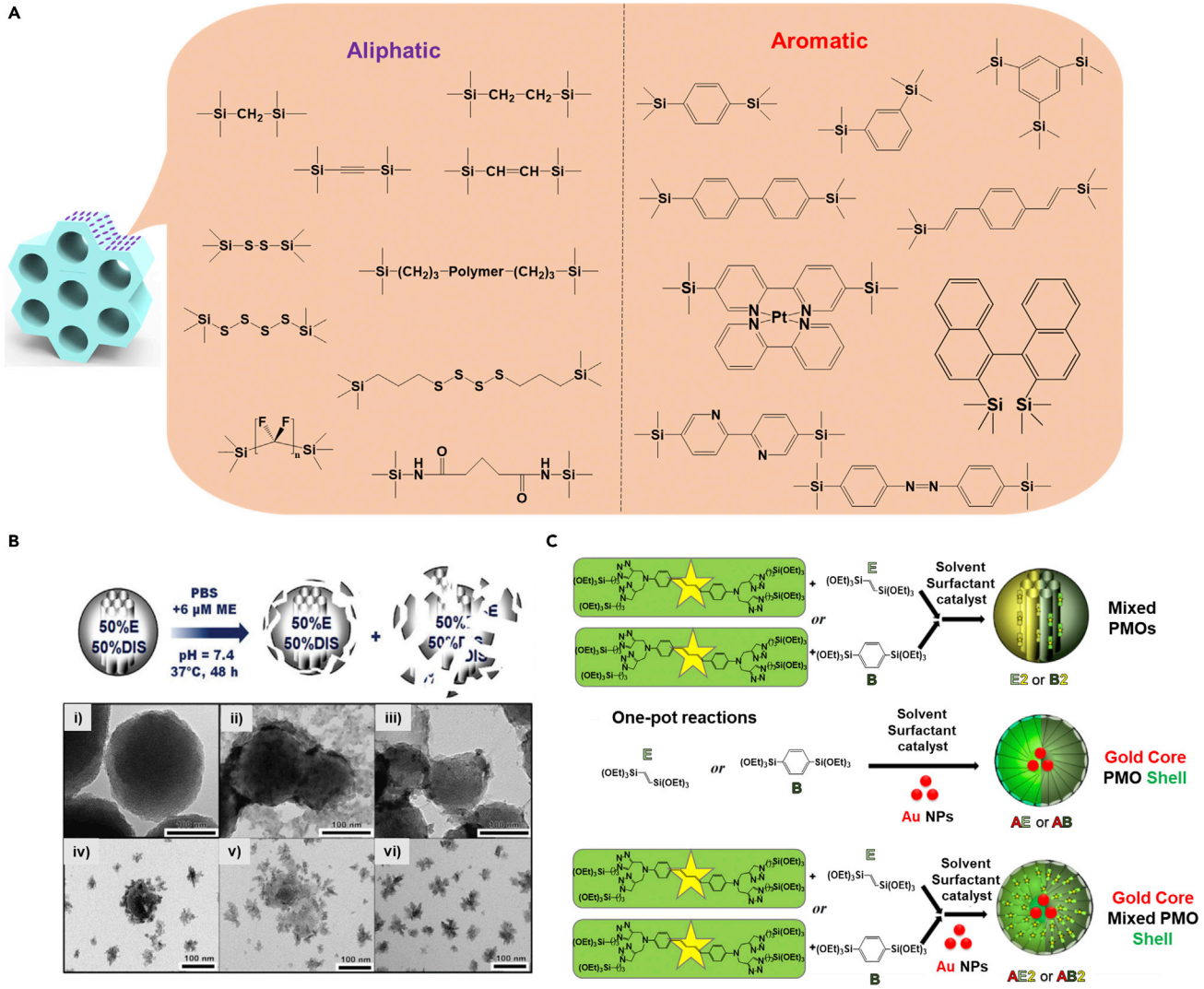

Figure 3. Fabrication of Biodegradable PMOs

(A) Schematic showing various organic (aliphatic and aromatic) functional groups installed in the siliceous nanoassemblies for advanced applications.

(B) Schematic illustration as well as transmission electron microscope (TEM) images are showing PMO nanospheres with mixed silanes in 50/50 before (i) and after 48 hr of degradability in the physiological conditions (ii–vi). Reproduced with permission from (Croissant et al., 2014a). Copyright 2014, John Wiley and Sons.

(C) Design of mixed PMO nanoparticles, composed of either bis (triethoxysilyl)ethylene, (E), or bis (triethoxysilyl)benzene (B), respectively; one-pot synthesis of AE or AB gold (Au) core-PMO shell nanoparticles, respectively, composed of either the E or B moiety; one-pot synthesis of AE2 or AB2 Au core-mixed PMO shell nanoparticles, composed of either 2PS and E (AE2) or 2PS and B (AB2 nanoparticles). Reproduced with permission from (Croissant et al., 2014b). Copyright 2014, American Chemical Society.

organic content in the MSNs would undoubtedly reduce the silanol density in the siliceous pool, facilitating their augmented degradability and compatibility attributes in the biological environment towards efficient delivery and diagnosis applications (Croissant et al., 2014a). Nevertheless, there also exist some contrary shreds of evidence on ethylene-bridged PMOs with an average size of ~20 nm, in which, despite their high hemocompatibility, these nanocomposites resulted in substantial resistance to degradation over pristine MSNs due to their ultrasmall sizes (Urata et al., 2011). To a considerable extent, the challenging task of biodegradability can be addressed by integrating with various organic groups, resulting in the uniform-sized PMOs (130–200 nm) with diverse morphologies ranging from sphere to rod for efficient drug delivery application. However, the organic groups with specific stimuli-responsive moieties within the organic groups would augment the degradation effects of MSNs. For instance, the mixture of bis (propyl)disulfide- and ethylene-bridged silanes at the ratio of 1:1 resulted in excellent biodegradability of resultant MSNs in

the physiological fluids and an augmented payload of guest species by altering the organosilane content (Figure 3B) (Croissant et al., 2014a). Despite the incorporation of organic moieties in MSNs, the degradation effect of the nanocomposites would be dependent on the disulfide bond (explicitly discussed in the disulfide/diselenide bridging section). However, it should be noted that the stringent optimization of drug loading characteristics and mechanisms of encapsulation, as well as substantial release, yet remained to be comprehensively explored. In addition, numerous efforts have been dedicated in addressing the biocompatibility of MSNs and their conjugates, specifically PMOs, not only in various human and animal cell lines (cancerous and noncancerous) and *in vitro* cell lines (HeLa, C2C12, A549, MDA-MB-231 LUC, MCF-41, 293T, L02) but also *in vivo* in animals and human red blood corpuscles (RBCs) to showcase the histocompatability and hemocompatibility, respectively (Croissant et al., 2014b, 2018; Guan et al., 2012). Notably, the compatibility of MSNs depends on the type of bridging groups incorporated in the siliceous frameworks. It was evident from the literature that the PMOs with various organic groups, such as methylene, ethylene, phenylene, benzene-porphyrin, and ethylene-butadienediphenyl groups, were compatible in MCF-7 and HeLa tumor cells (Croissant et al., 2014b; Guan et al., 2012). These PMO-based frameworks over the metal constructs as the shell had also offered excellent compatibility in MDA-MB-231 LUC cells at well-tolerated doses. One of the predominant reasons for the compatibility of these nanocomposites might be due to the rapid coating of the proteins *in vivo*, resulting in improved biocompatibility of MSNs. In addition to the bridging groups, the other parameters such as morphology and aggregation would play essential roles in the cytotoxicity of PMOs, in which the PMO-based nanorods and nanowires were comparatively lesser toxic over the sphere-shaped particles (Fatieiev et al., 2017).

Furthermore, the impregnated organic species that offer the biodegradable feature to MSNs not only deliver the therapeutic guest species but also assist in the stimuli-responsive switching mechanism, which could be considered even with no additional capping agents (Croissant et al., 2014a). In this framework, incorporating a mixture of organosilane precursors, *i.e.,* bis (triethoxysilyl)ethylene, (E), or bis (triethoxysilyl)benzene (B), would result in high specific surface areas that could enable augmented therapeutic cargo conveying ability and synergistic therapeutic effects (Figure 3C) (Croissant et al., 2014b). Interestingly, the accommodated organic bridges in the siliceous frameworks offer the formation of a new type of the molecular-scale ordering of pore walls with regular packing and long-range order of the columnar assemblies (Croissant et al., 2015b; Mizoshita and Inagaki, 2015). In this regard, such organic species-doped MSNs might enable the alteration of morphological attributes and improvement in various physicochemical characteristics of MSNs, in which the hydrogen-bonded organosilicas facilitate establishing the interactions with the guest species toward improved encapsulation of diverse guest species (Croissant et al., 2015b). Despite their success in fabrication, it is highly challenging to regulate the porosity and the morphology, as well as the organization of silsesquioxane species in PMOs. However, several attempts of adding organoalkoxysilane to silica precursors often resulted in a deprived quantity of the organic content, affecting their biodegradable and morphological properties (Croissant et al., 2016a).

Disulfide/Diselenide Bridging

Despite the enormous efforts, there exist specific contradictory perspectives on the biosafety of MSNs owing to the lack of detailed insights because of complex biological environments and challenges of imaging technologies. To this end, the degradation and colloidal stability attributes of nanocarriers are the essential requirements for the *in vivo* clearance of MSNs, determining their safety and eventual fate in the physiological environment (Wang et al., 2019c). However, it should be noted that the degradability of MSNs firmly depends on the degree of hierarchical framework condensation, morphological attributes, and immobilized chemical functionalities, among others (Du et al., 2018a; Wu et al., 2018). Comparatively, the silicon-based porous nanomaterials display higher dissolution in the aqueous environment over MSNs due to successive hydrolysis reactions. Nevertheless, this uncontrolled degradation property may not be the most desirable characteristic feature for their application *in vivo* as they may lead to toxicity risks. Conclusively, the small-sized silica particles with poor degradability behavior may be better than the materials with uncontrolled degradation behavior for biomedical applications (Prasetyanto et al., 2016). Considering these facts, precise re-engineering of siliceous frameworks that can achieve controlled degradation in the specific microenvironment alongside exhibiting the therapeutic effects is desirable (Maggini et al., 2016; Yang et al., 2016b). Indeed, one of such environments is the intracellular reductive microenvironment that with enriched glutathione (GSH) content enables the redox-triggered biodegradation of hybrid materials installed with disulfide or thioethers, such as bis (propyl)disulfide, (- $(CH_2)_3$-S ~ S- $(CH_2)_3$-) and bis (propyl)tetrasulfide (- $(CH_2)_3$-S ~ S ~ S ~ S- $(CH_2)_3$-), or diselenide-bridged moieties (Figures 4A and 4B) (Du et al., 2018b; Kankala et al., 2020a; Kim et al., 2012; Quesada et al., 2013; Shao et al., 2018; Teng et al., 2014).

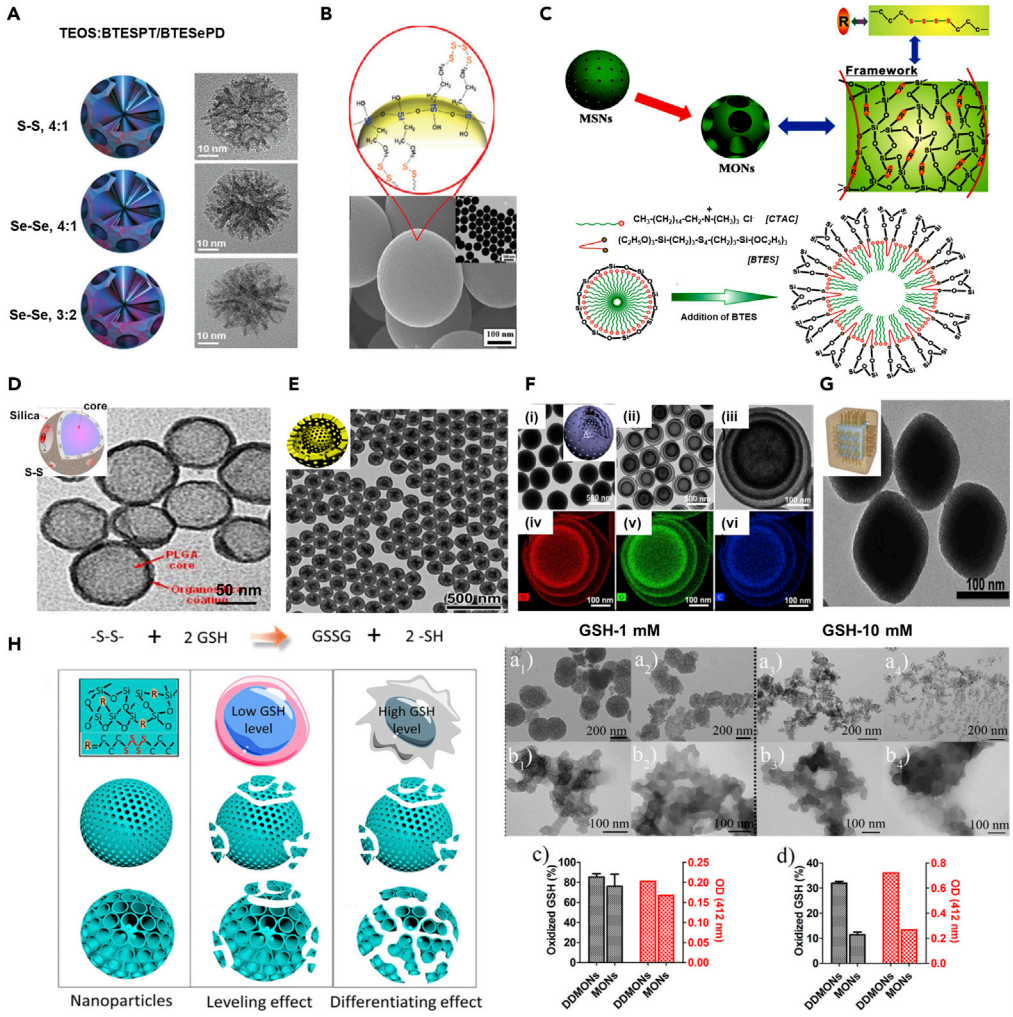

Figure 4. Disulfide/Diselenide-Bridged Organosilica Hybrid Constructs

(A) Reconstructed three-dimensional (3D) models and corresponding TEM micrographs of disulfide/diselenide-bridged organosilica constructs. Reproduced with permission from (Shao et al., 2018). Copyright 2018, John Wiley & Sons.

(B) Schematic showing the arrangement of disulfide bridging over the solid MSNs. Reproduced with permission from (Kim et al., 2012). Copyright 2012, American Chemical Society.

(C) Schematic representation for the CTAC-based molecularly organic-inorganic hybrid composition of thioether-bridged mesoporous organosilicas. Reproduced with permission from (Wu et al., 2015). Copyright 2015, John Wiley & Sons.

(D) Electron microscopy image of hybrid PLGA@organosilica nanoparticles. Reproduced with permission from (Quesada et al., 2013). Copyright 2013, American Chemical Society.

(E) TEM image of the yolk-shell mesoporous nanoparticles with thioether-bridged organosilica frameworks prepared by hydrothermal treatment. Reproduced with permission from (Teng et al., 2014). Copyright 2014, American Chemical Society.

(F) (i–iii) Triple-shelled PMO hollow spheres with ordered radial mesochannels prepared by a one-step hydrothermal treatment of the organosilica spheres with different growth cycles (iv-vi) and their corresponding EDX elemental mapping images. Reproduced with permission from (Teng et al., 2015). Copyright 2015, American Chemical Society.

(G) TEM image of Prussian blue-based core-shell thioether-bridged organosilica architectures. Reproduced with permission from (Tian et al., 2017). Copyright 2017, John Wiley & Sons.

(H) Schematic showing the pore structure-dependent degradability of nanoparticles within healthy and cancer cells. Degradation test of degradable dendritic mesoporous organosilica nanoparticles (DDMONs) (a1-a4) and mesoporous organosilica nanoparticles MONs (b1-b4) tested at 1 and 10 mM GSH solution in the presence of serum and (c and d) their corresponding enumerated outcomes. GSH oxidation percentage (black columns) and relative quantity of –SH groups after incubation of DDMONs or MONs in GSH solution in the presence of serum. Reproduced with permission from (Yang et al., 2016b). Copyright 2016, American Chemical Society.

In this context, Shi and colleagues fabricated thioether-functionalized mesoporous nanocomposite frameworks through a one-step condensation approach (Zhang et al., 2003). Further, these frameworks have been successfully used in diverse applications, including medicine and catalysis (Croissant et al., 2014a; Du et al., 2014, 2018a; Zhou et al., 2017). Relatively, the disulfide linkages installed in MSNs are more stable in the neutral pH conditions, equivalent to physiological fluids or bloodstream compared to those of organic moiety-doped siliceous frameworks, such as PMOs. However, these are highly sensitive to the reductive environment through a disulfide-thiol exchange reaction, facilitating the release of therapeutic guest species (Croissant et al., 2014a; Kankala et al., 2019; Zhou et al., 2017). Thus, the molecular responsiveness has become one of the most promising stimuli-triggered strategies in cancer therapy, due to various reasons of the presence of higher levels of GSH in cancer cells over healthy cells, high replenishment of intracellular GSH levels, and presence of redox-active moieties, such as thiol reductase and cysteine levels in the endosome/lysosome organelles (Du et al., 2018a; Hadipour Moghaddam et al., 2018). Initially, the reductive ability of the disulfide/diselenide linkage was applied for the mesopore opening mechanism, which, however, explored for nanoarchitecting the biodegradable frameworks in addressing the biosafety concerns of silicas along with PMOs (An et al., 2016; Quesada et al., 2013). In this vein, several efforts have been dedicated in recent times to demonstrate the efficacy of disulfide/diselenide-bridged mesoporous frameworks for cancer drug delivery and the biocompatibility of these responsive frameworks even at high doses (Huang et al., 2017; Wu et al., 2015). Comparatively, the stimuli-responsive diselenide linkage is more advantageous owing to its lower bond energy of 240 kJ/mol and relatively weaker electronegativity over disulfide bond (172 kJ/mol), indicating its susceptibility to the reductive environment (Shao et al., 2018).

In addition to various commercially available thioethers (- $(CH_2)_3$-S_4 (or S_2) - $(CH_2)_3$) (Figures 4B) (Kim et al., 2012), several smart designs of customized disulfide-bridged silanes have been used to fabricate disulfide-bridged silsesquioxane frameworks based on sol-gel type self-assembly approach. Notably, the hydrophobicity of the organic chain often limits the condensation of silica, affecting the cooperative self-assembly, which could be addressed by premixing the thioether substrate with the silica precursor. Since ever the first report (Zhang et al., 2003), numerous varieties of disulfide-bridged siliceous frameworks with varying sulfur amounts have been fabricated, including diverse morphologies of non-porous solids, hollow/core-shell/yolk-shell architectures, and structures with radial pores (Hadipour Moghaddam et al., 2018; Kim et al., 2012; Quesada et al., 2013; Teng et al., 2014; Wu et al., 2015). Such progressions led to significant changes in the resultant siliceous frameworks, including the order of addition and hydrophilicity in the silylated precursor. Premixing of disulfide precursors containing a silylated component with tetraethyl orthosilicate (TEOS) often ends up with a high amount of disulfide-bridged silsesquioxane content at ease, which, however, also results in the reduction of the final size of mesopore (Du et al., 2018a). Moreover, the disulfide component containing a silylated precursor with more hydrophilicity often results in well-structured architectures with ordered pores. At the same time, the presence of longer hydrophobic chains leads to interaction with the hydrophobic part of the surfactant during the self-assembly, resulting in the irregular architectures with inevitable structural changes (Croissant et al., 2014a; Du et al., 2018a).

Indeed, the well-ordered MSN-based hybrid architectures with appropriate sulfur content have been fabricated by regulating the experimental conditions using the cooperative self-assembly approach based on sol-gel chemistry. Interestingly, the ultrasmall-sized (~30 nm), large pore (8–13 nm) disulfide-bridged siliceous frameworks can be fabricated through penetrating the long hydrophobic chains into the gaps of the hydrophobic part of the structure-directing agent (for instance, cetyltrimethylammonium chloride, CTAC) micelles (Figure 4C) (Wu et al., 2015). In addition, several progressions include the fabrication of hollow/core-shell/yolk-shell/rattle-type mesostructured nanoarchitectures with disulfide bridging moieties. These architectures can be fabricated using a self-template selective etching approach based on silica and other templates such as hard templating approaches of block polymers and Prussian blue, among others, resulting in the yolk-shell, as well as multi-shelled, disulfide-bridged nanoarchitectures (Figures 4D–4G) (Quesada et al., 2013; Teng et al., 2014, 2015; Tian et al., 2017). Notably, the hydrothermal treatment during fabrication often results in nanocomposites with deprived degradation ability due to the high degree of silica condensation. Attempts of scale-up production of these hollow siliceous architectures have also been made, whose applicability is yet limited due to severe aggregation (Huang et al., 2017). Nevertheless, compared to disulfide-bridged hierarchical siliceous architectures and non-porous structures, the hollow/core-shell/yolk-shell/rattle-type mesostructured nanoarchitectures with disulfide bridging, which coated over a functional entity, offered a significant advantage of enhancing GSH-triggered biodegradation.

Remarkably, this behavior of disulfide bridging is highly controllable as the GSH levels are high in cancer cells over normal healthy cells that accompany drug release, as well as protection to healthy cells from these foreign bodies (Figure 4H) (Yang et al., 2016b).

Moreover, the stimuli-responsive degradation ability of disulfide/diselenide bridging moieties in MSNs offers a complete release of the encapsulants from the mesopores, facilitating their rapid elimination from the body. Although these hybrid species offer degradation ability, it firmly depends on the surface area of exposure of GSH species to the disulfide-bridged frameworks. In some instances, the mesoporous frameworks with small-sized pores could be blocked by the serum proteins, in which the exposure of disulfide linkage to access by GSH is inhibited. Therefore, the large-sized HMSNs are highly favorable for cancer-specific delivery of therapeutic guests (Yang et al., 2016b). Despite the rapid and controllable degradation ability for better therapeutic efficacy by accelerating the release of the encapsulated therapeutic cargo, the degraded products of disulfide-/diselenide-bridged MSN frameworks may cause the significant biosafety concern. To achieve this, several steps are required to be taken in terms of monitoring the degradation profile, characterizing the degraded products, requiring detailed mechanistic insights of redox-triggered degradation, and dose optimization to overcome the tolerance threshold due to the rapid degradation and *in vivo* clearance.

Doping Metal Species

Despite their intrinsic colloidal, thermal, and mechanical stabilities, as well as low density, the applicability of these unique porous materials, in diverse fields, specifically adsorption, biomedicine, and catalysis, is often limited due to the amorphous and neutral character of pure silica (Aspromonte et al., 2012). In a way, this could be addressed by incorporating diverse metal species (divalent and trivalent cations) in the siliceous pool, leading to the reduced concentration of the silanol groups and additional properties offered by contrarily charged species, which are of specific interest for their applicability in diverse fields (Kankala et al., 2015; Kuthati et al., 2017). In recent times, tremendous progress has been evidenced by the utilization of diverse metal species, including first-row-transition metals, *i.e.*, iron (Fe), cobalt (Co), nickel (Ni), copper (Cu), and zinc (Zn), toward fabricating highly efficient metal-doped nanocomposites for addressing some of the aforementioned bothering precincts of MSNs (Kankala et al., 2015; Parvulescu and Su, 2001). Incorporating such metal species augment the physicochemical features of MSNs, for instance, aluminum, which significantly enhances the surface acidity and chemical functionality of alumina to siliceous frameworks, leading to enhanced performance efficiency of the nanocomposites (Cesteros and Haller, 2001; Chen et al., 1993; Corma et al., 1994; Eimer et al., 2002; Huo et al., 2014; Kolodziejski et al., 1993; Monnier et al., 1993; Ryoo et al., 1997). Nevertheless, specific essential facts of dependency in terms of formulation factors should be predominantly considered while fabricating the metal-species-encapsulated MSNs. The major formulation aspect of determining optimal reactant concentration of metal species concerning the silica amount plays a crucial role as the inappropriate amounts of metal may lead to either alteration of the mesoporous frameworks, resulting in the irregular shaped structures, or deposition of corresponding metal oxide constructs in the mesopores (Aspromonte et al., 2012). On the other hand, the processing features, such as pH of the reaction and type of solvent, also affect the formation of MSNs, leading to ease of oxidation and resulting in the separation of corresponding metal oxide composites, for instance, Fe species in the presence of ammonia (Yonemitsu et al., 1998). In addition, the alignment of mesopores while arranging the metal species must be considered such that the deposition of metals in the siliceous frameworks would not influence the formation of deep mesopores with large pore volume, which may substantially affect the encapsulation efficiency of therapeutic guest species in the mesopores (Kankala et al., 2017; Parvulescu and Su, 2001).

Comparatively, it is more convenient to incorporate metal species in the siliceous pool of the MCM-41-based materials over Santa Barbara Amorphous (SBA)-type constructs. In this context, the utilization of quaternary ammonium surfactants as templates in the fabrication of MCM-41 species can conveniently accommodate the metal cations (Cu, Fe, and Zn) through electrostatic interactions. Contrarily, the metal species in their nanoparticulate forms (metal nanoparticles, MNPs) could be deposited more favorably in the highly ordered mesopores of SBA-15 species. Notably, the accommodated metal species in the mesopores would show no significant influence on the morphological attributes of the composites, yielding ultra-fine, discrete nanoarchitectures with enriched physicochemical characteristics. In this regard, the transition metals (divalent and trivalent species, specifically Cu (II), Zn (II), and Fe (III)) encapsulated in the MCM-41 species through the traditional condensation approach facilitate the establishment of stable

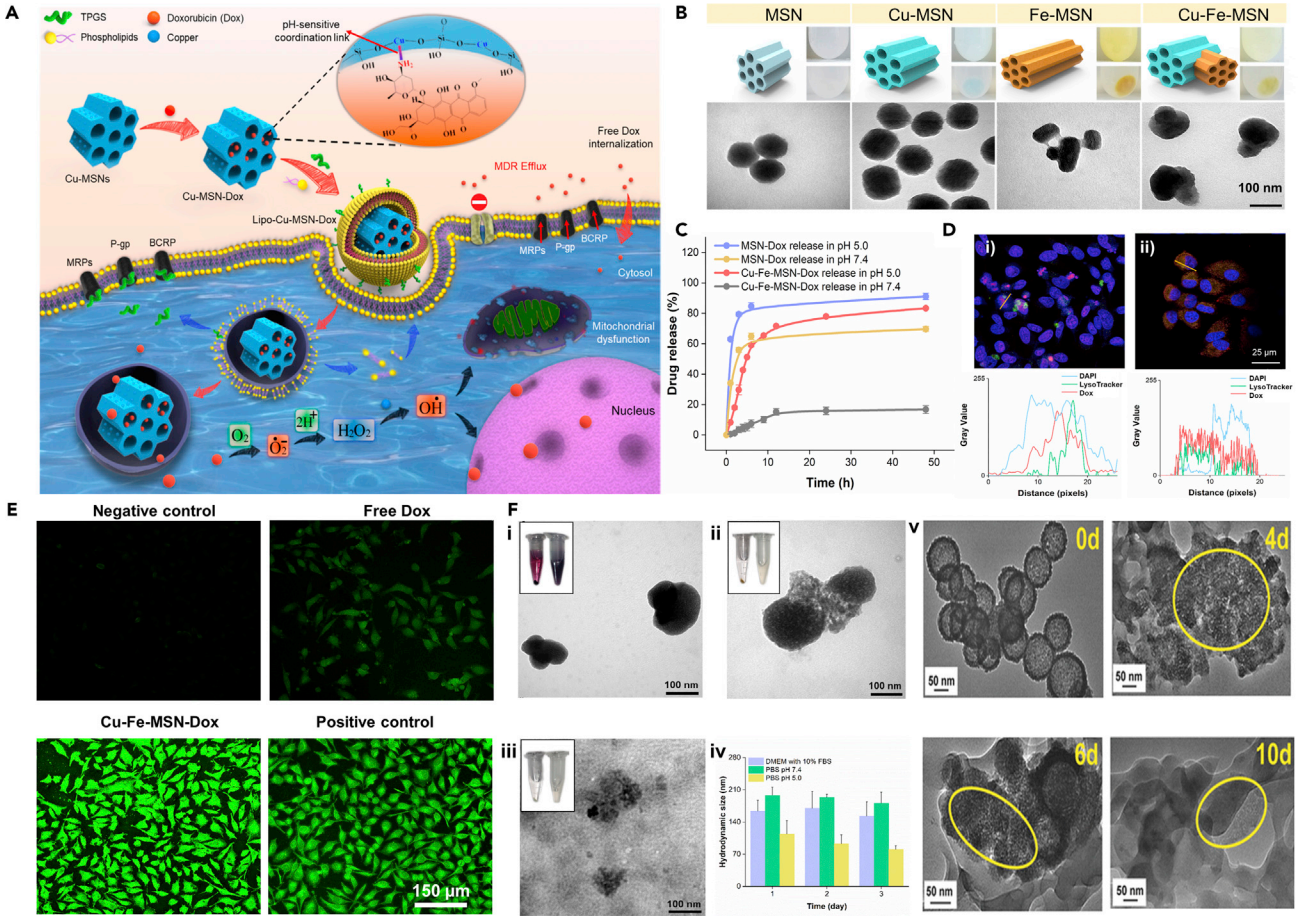

Figure 5. Metallic Linkers in the Siliceous Frameworks for Diverse Biomedical Applications

(A) Schematic illustration showing the synthesis of designed hierarchical metal-impregnated MSNs elucidating the mechanistic illustration of pH-responsive delivery of a drug in the tumor environment. Reproduced with permission from (Kankala et al., 2017). Copyright 2017, American Chemical Society.

(B) Illustration showing the fabrication of various metal-doped MSNs along with the structures elucidating the arrangement of transition metals in the silica wall and their corresponding optical sample images, as well as TEM micrographs.

(C) pH-responsive release of doxorubicin (Dox) from Cu-Fe-MSNs in vitro at various time intervals in the simulated fluids, compared to naked MSNs.

(D) Cellular internalization illustrating the lysosomal escape of free Dox and Cu-Fe-MSN-Dox in HeLa cells and their respective RGB fluorescence intensity profiles of DAPI, LysoTracker, and Dox at the selected region (yellow line) from the samples, (I) Free Dox, and (ii) Cu-Fe-MSN-Dox, respectively.

(E) Confocal laser scanning microscope (CLSM) images are showing the ROS levels correlating to 2′,7′-dichlorofluorescein diacetate (DCF-DA) fluorescence in HeLa cells after treatment with bare MSNs, Cu-MSNs, Fe-MSNs, Cu-Fe-MSNs, and Cu-Fe-MSN-Dox.

(F) Degradation of Cu-Fe-MSNs in vitro in (i) media with 10% serum and phosphate-buffered saline (PBS), (ii) pH-7.4, and (iii) pH-5.0. (the inset box showing the optical images of samples after centrifugation on left and dispersion, of the respective sample on right) (iv) Hydrodynamic sizes of Cu-Fe-MSNs in 10% serum-containing media and PBS. Reproduced with permission from (Liu et al., 2019). Copyright 2019, Elsevier. (v) TEM images of Fe-HMSNs after the biodegradation in serum. Reproduced with permission from (Wang et al., 2017). Copyright 2017, John Wiley and Sons.

coordination interactions with the theranostic guest species (Figures 5A and 5B) (Kankala et al., 2015, 2017; Liu et al., 2019). The doped metal species, for instance, Cu species, are generally arranged axially within the siloxyl assemblies of MSNs, confirmed by the electron spin resonance studies. Such established interactions offer enormous benefits, including the augmented encapsulation efficiency of diverse guest species, precise delivery at the target site, and participation in the synergistic therapeutic effects for better therapeutic outcomes (Figures 5C and 5D) (Kankala et al., 2015, 2017, 2020b). Oftentimes, these interesting features have been demonstrated by various approaches of capping mesopores using polymeric or protein assemblies over the MSN surface (Croissant et al., 2016b; Niedermayer et al., 2015; Zhang et al., 2015b) or quantum dots and MNPs on mesopores using the stimuli-responsive linkages (Chen et al., 2016; Yang et al., 2016a), which often require multi-step preparation procedures, resulting in distortion of MSN shape due to mechanical abrasion (Liu et al., 2019). Further, the precise release of encapsulated guest species in

the acidic environment would enable their effective conveyance in the physiological stream by avoiding the premature release and attaining the required therapeutic levels at the target site. Such targeted release leads to an effective therapeutic outcome by minimizing the side effects through precise control over the on-demand release of therapeutic guest molecules.

The encapsulated transition metals (cationic species) in the siliceous frameworks can significantly alter the net negative charge of MSNs, facilitating the cellular internalization efficiency through improving the interactions with the negatively-charged biological membranes (Kankala et al., 2015). However, this approach is often limited to drug molecules with specific functionalities, for instance, amine-based drugs, in which the acidic pH assists in their selective protonation, resulting in the disassembly of the metal-ligand interactions (Kankala et al., 2017, 2020b; Kuthati et al., 2017). Owing to the sensitivity of the coordination interactions between the host and guest species, specifically in the acidic environment, these metal-doped MSNs are predominantly applicable for the delivery of chemotherapeutics and antibiotics. Moreover, such metal-doped mesoporous nanoarchitectures can be used in nanomedicine as they successfully contribute to synergistic therapeutic effects. Apart from the cellular internalization facilitated by the unique electronic arrangement contributed by the surface charge, the incorporated metal species in the siliceous frameworks work a step beyond as nanoreactors (Kankala et al., 2015). The highly functional nanomachinery, precisely a few of the first-row-transition metals, Cu and Fe, efficiently works by transforming the naturally available hydrogen peroxide (H_2O_2) molecules. Specifically, the higher levels of H_2O_2 in cancer over healthy cells could lead to the overproduction of deadly reactive oxygen species toward significant ablation of tumors, referring to chemodynamic therapy (Figure 5E) (Liu et al., 2019). In recent times, we have attempted to incorporate multiple metal species (Cu and Fe) in the mesoporous frameworks, resulting in the altered shape owing to the repulsions of the transition metal species (Liu et al., 2019). Interestingly, the increased metal species with reduced siloxyl content in MSNs augmented the biodegradability of silica frameworks, enabling through the disassembly of the transition metal-based coordination interactions (Figure 5F-i-iv) (Liu et al., 2019). In another case, the incorporation of Fe species alone in the mesoporous architectures also facilitated the unique chemical coordination-accelerated biodegradation (Figure 5F-v) (Wang et al., 2017). Despite the advantageous physicochemical attributes, doping multiple metal species in the siliceous frameworks requires critical optimization in terms of the arrangement of different metal in the siliceous pool, compatibility, optimization of concentration, as well as appropriate ratio of metal species, and various mechanisms reconnoitering their applicability yet to be explored (Kuthati et al., 2017).

Shaping

With the application requirements as the utmost importance, the well-ordered geometries and eventual shapes of highly rigid MSNs can be altered, resulting in the development of unconventional, cutting-edge asymmetric constructs, as well as biologically or nature-inspired nanoarchitectures. In addition to the change in shapes, the overall morphology can be adapted from traditional hexagonal to different shaped constructs such as disordered, lamellar, cubic, and wormhole-like constructs by regulating the synthesis conditions, such as altering the ratio of the surfactant to the silica precursor and surfactant template (Argyo et al., 2014; Slowing et al., 2008). Notably, in the synthesis of the hollow-type MSNs, the core-shell composites of silica could act as precursors in fabricating some of the nature-mimicking constructs, such as peanut-, rattle-, flower-shaped architectures by selectively altering the etching agent from sodium carbonate to ammonia and monitoring its concentration as well (Wang et al., 2013). Among the modified siliceous frameworks, the anisotropic and nature-inspired nanoarchitectures, including multi-podal and flower-shaped nanoassemblies, are the recent innovative progressions toward their applicability in biomedical and catalysis fields.

Janus-type Nanoarchitectures

Given improving the essential functionalities, stability, and physicochemical attributes of the traditional siliceous frameworks, various anisotropic hybrid architectures, commonly referred to as Janus-type constructs, are fabricated (Sánchez et al., 2013; Shao et al., 2016; Villalonga et al., 2013). More often, these asymmetric constructs with well-defined particle sizes and controlled shapes can be fabricated by utilizing multiple first-row-transition metal species, upconverting nanoparticles (UCNPs) (Li et al., 2014), and other metals such as platinum (Pt) and gold (Au) (Ma et al., 2015; Sánchez et al., 2013; Xuan et al., 2016). These structures with the altered charge densities, as well as extensive surface properties, display improved magnetic, electrical, and optical characteristics over the conventional MSNs (Xuan et al., 2016). Nevertheless, it is worth noting that the composition and crystal assemblies of the utilized components and eventual

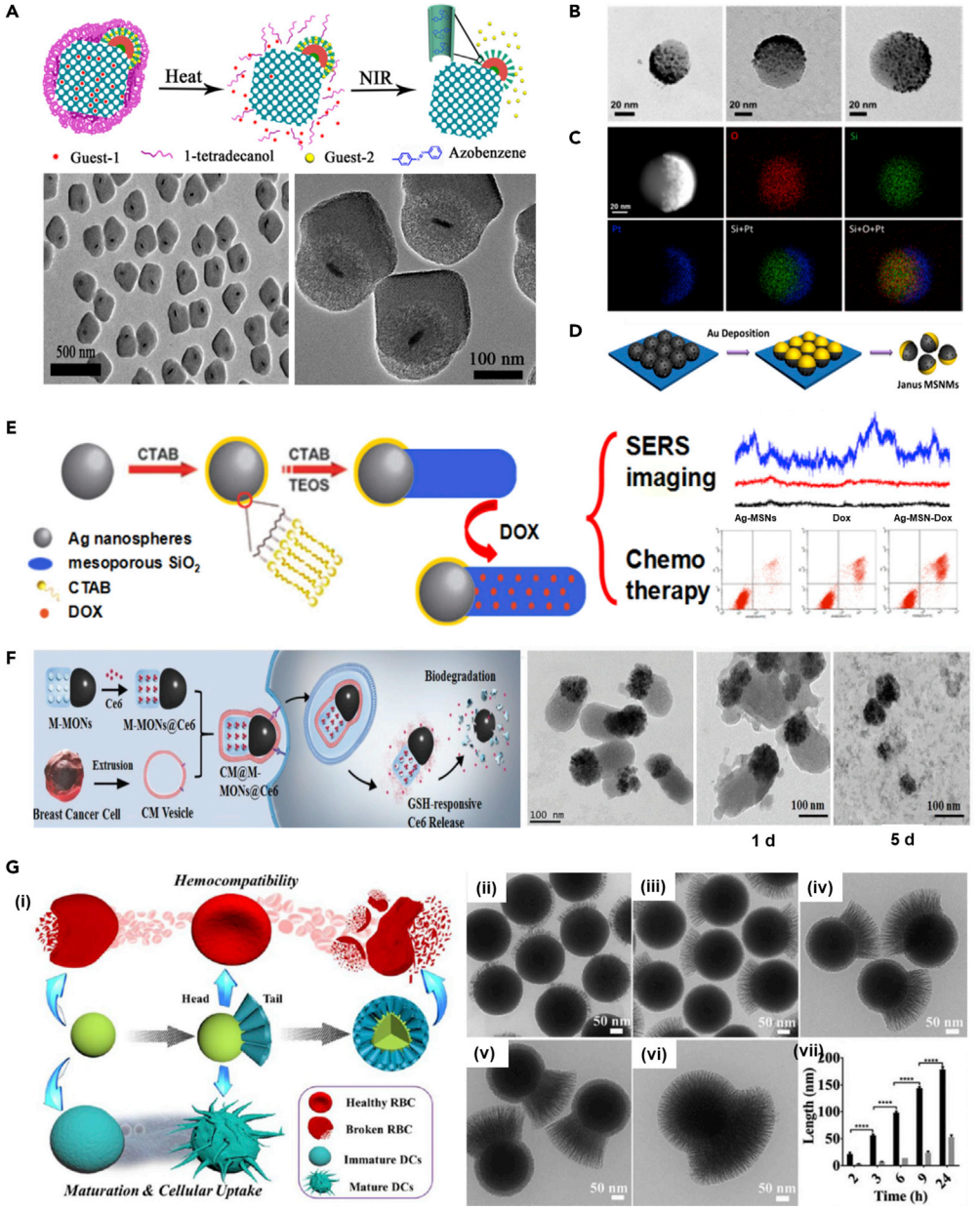

Figure 6. Janus-Type Nanoconstructs for Advanced Biomedical Applications

(A) Dual compartment Janus MSNs, UCNP@Si O $_2$@ mSi O $_2$&PMOs by the anisotropic island nucleation and growth method (UCNP = NaGdF4:Yb,Tm@NaGdF4, mSi O $_2$ = mesoporous silica shell) and their corresponding TEM images. Reproduced with permission from (Li et al., 2014). Copyright 2014, American Chemical Society.

(B) Characterization of Janus MSNs with different sizes coated with Pt (2 nm) by electron beam deposition.

(C) High-angle annular dark-field–scanning TEM (HAADF-STEM) image and element mapping of Janus MSNs. Reproduced with permission from (Ma et al., 2015). Copyright 2015, American Chemical Society. Note: Further permissions related to the material excerpted should be directed to the American Chemical Society.

(D) Schematic illustration of Au nanoparticle-coated Janus MSNs by vacuum sputtering. Reproduced with permission from (Xuan et al., 2016). Copyright 2016, American Chemical Society.

(E) Schematic showing the fabrication procedure for the Dox-loaded Ag-MSNs and their application towards SERS imaging and pH-sensitive drug delivery in cancer therapy. Reproduced with permission from (Shao et al., 2016). Copyright 2016, American Chemical Society.

(F) Schematic showing the synthetic procedure for the Janus magnetic mesoporous organosilica nanoparticles and their application for combined PDT and magnetic hyperthermia. TEM images of constructs showing the selective degradability

Figure 6. *Continued*
behavior in 5 × 10^{-3} m GSH solution for 1 and 5 d. Reproduced with permission from (Wang et al., 2019c). Copyright 2019, John Wiley & Sons.
(G) (i) Schematic illustrating the synthesis of Janus MSNs and their advantages in hemocompatibility and maturation of immune cells. (ii-vi) TEM images (A–E) of Janus MSNs 1.25-t-60 collected at different reaction times (t = 2, 3, 6, 9, and 24 hr, respectively). (vii) Variation of tail length (black bar) and head coverage (gray bar) as a function of t. Bars represent the mean ± SEM (n = 20). Reproduced with permission from (Abbaraju et al., 2017). Copyright 2017, American Chemical Society.

deposition of silica over them significantly influence the final shape of the Janus-type nanocontainers. Compared to conventional Janus structures based on polymers or silica, the MSNs-based composites can facilitate improved applicability in medicine, in terms of conveying and delivering enhanced loads of multiple chemotherapeutic agents and powered movement in physiological fluids, among others (Karimi et al., 2017; Li et al., 2014).

In this vein, numerous strategies have been applied for engineering these "so-called" Janus-type nanoarchitectures (Abbaraju et al., 2017). In a case, chemically powered synthesis was utilized to fabricate innovative Janus-type, asymmetric architectures with UCNPs (NaGd-F4:Yb,Tm@$NaGdF_4$) as cores and dual independent mesophases as shells. The synthesis approach assisted with the mechanisms of anisotropic heterogeneous island nucleation and growth, resulting in the anisotropic growth of silica over the UCNPs for the delivery of dual drugs (Figure 6A) (Li et al., 2014). In addition, other facile routes, such as surfactant templating, Pickering emulsion-assisted, and chemical-based strategies, have been applied to deposit various MNPs, such as silver (Ag), Au, and iron oxide constructs, toward fabricating the Janus-type architectures through distinct functionalization chemistries (Ma et al., 2015; Shao et al., 2016). Owing to their characteristic surface properties, the inorganic MNPs-deposited Janus architectures with net driving force could act as nanomotors under external forces such as the magnetic field or enzyme-controlled sensing actuation through bubble propulsion mechanism for stimuli-responsive therapeutic cargo delivery, biosensing, and biocatalysis applications (Villalonga et al., 2013).

Several attempts of asymmetric capping by utilizing organic molecules, for instance, phenyltriethoxysilane, have also been made through well-defined functionalization chemistries, which resulted in the hemispherical organic shell (Ujiie et al., 2015). Although the utilization of organic linkers is advantageous toward overcoming the problems of inorganic composites, however, the hybrid materials using organic and inorganic species would suffer from their specific limitations while applying in medicine and phase-selective catalysis. In another instance, the controlled synthesis of PMOs using *p*-isomer of phenylene-ethylene by the facile sol-gel process at a slow stirring speed resulted in the Janus-type nanoconstructs with multipods, in which the *p*-isomer of the precursor was effective as a substrate than the *m*-isomer (Croissant et al., 2016a). Notably, these constructs with higher molecular periodicity offered excellent thermostability and augmented therapeutic cargo-carrying attributes. In this vein, diverse physical strategies such as vacuum sputtering and electron beam evaporation have been utilized for fabricating the Janus-type architectures (Ma et al., 2015; Xuan et al., 2016). These approaches predominantly resulted in the hemispherical structures owing to the uneven deposition of metal species either as irregular metallic islands (Figure 6B) or precise cap-like structures on the surface of MSNs (Figures 6C and 6D) (Ma et al., 2015; Xuan et al., 2016). Interestingly, these uneven metal islands would also empower them toward motor activities, referring to self-thermophoresis, for nanocatalysis, surface-enhanced Raman scattering imaging (Figures 6E) (Shao et al., 2016), and targeted drug delivery applications assisted with the biodegradable siliceous frameworks (Figure 6F) (Wang et al., 2019c). Nonetheless, the challenges of limited cargo loading efficiencies, damage of encapsulated thermosensitive molecules, and deprived safe transportation at high speed in biological fluids might limit their applicability. Integrating certain molecular gatekeepers on the mesopores could protect the encapsulated cargo to a considerable extent. Moreover, the growth of the randomly distributed islands is highly challenging in regulating the surface attributes of Janus architectures. Despite the success in fabricating such versatile Janus-type nanoarchitectures, the shortcomings such as multi-step fabrication procedures, biocompatibility, and biodegradability issues would limit their applicability. In an attempt to solve these issues, we demonstrated the fabrication of Janus-type (sphero-ellipsoid) architectures using a facile approach of doping dual metals, Cu and Fe, in the siliceous frameworks (Liu et al., 2019). Incorporating a couple of first-row-transition metal species with positive charges on the pre-MSN core resulted in the change of MSN shape, which could be due to the repulsive forces between the metal species while accommodating in the MSNs. Additional advantages offered by the incorporated

transition metals in the silica pool include improved drug encapsulation and programmed delivery, as well as contributing to the synergistic tumor ablation effect (Kankala et al., 2015, 2017, 2020c; Kuthati et al., 2017; Liu et al., 2019). Notably, these asymmetric structures with controllable shapes could provide excellent compatibility at the cellular level *in vitro*, as well as hemocompatibility and maturation of immune cells, which drove their applicability towards medicine (Abbaraju et al., 2017) (Figure 6G).

Multi-Podal Architectures

Multi-compartment nanoparticles with controlled and diverse morphologies in terms of shape and size offer enormous advantages owing to their influence on final electrical, optical, and physicochemical properties, as well as applicability in diverse fields (Sun and Xia, 2002). It should be noted that regulating the operating conditions and the concentrations of the substrate, as well as the structure-directing agent, would substantially alter the overall morphology of the resultant MSNs. In a way, varying the concentration of the organosilane precursor could result in the diverse morphologies ranging from the spheres to micron-sized needles and stars owing to the molecular ordering of the substrates and cooperative self-assembly of the structure-directing agent (Figure 7A) (Croissant et al., 2016a). In another case, the formation of auxiliary elements called pod-like structures with radial porosity happened to be favorable by lowering the stirring speed. These branched hetero-nanostructures with high morphological complexity based on anisotropic nanoassemblies have been recently reported using colloidal clusters of silica. For instance, the first classic example of fabricating the silica-based multi-podal architectures was by Wiesner and colleagues. They demonstrated that the two-dimensional (2D) hexagonal silica pods were installed onto the silica core with cubic porosity through epitaxial growth (Suteewong et al., 2013). Further, it could also be feasible to fabricate crystal-like PMO-based multi-podal architectures with one to eight pods of ethylene-bridged on the benzene-bridged PMO cores toward enhanced characteristics using a one-pot, two-step process (Figure 7B) (Croissant et al., 2015a). Interestingly, the multiple rod-shaped pods were fabricated, being one or two pods most among all. In the case of introducing components with various functionalities in the core and pods separately similar to the irregular Janus-type constructs, these innovative structures could be applied for catalysis, photonic, and biomedical applications. These multi-compartment nanocontainers with selective drug adsorption could be applied for multidrug delivery. Notably, the dendritic fibrous nanosilicas that look similar to multi-podal structures can be used as effective templates toward the fabrication of mesoporous silica and metal-based hybrid core-shell nanocomposites, offering numerous catalytically active sites compared to conventional MSNs and metal-impregnated MSNs (Byoun et al., 2018). Detailed insights on the dendritic or fibrous MSNs are given in the section of flower-shaped packing.

Despite the progressions in fabricating highly complex multi-compartment models, the precise modification and efficient control over the surface topology while nanoarchitecting the siliceous frameworks are highly challenging. Inspired by the virus invasion to the cell membrane through the multipod-like spikes, the surface of the MSNs was regulated by controlling the multiple nucleation sites toward fabrication of precisely controllable structures on the surface. Accordingly, Janus one-pod to multiple ranging from two-, three- and Tribulus-like tetra-pods at arbitrary dimensions can be fabricated. In an attempt to achieve this aspect, Zhao and colleagues demonstrated the precise control over the nucleation number of PMOs over the surface of resorcinol-formaldehyde resin core, yielding multi-podal core@shell nanospheres (Figure 7C) (Zhao et al., 2019). Contrary to the traditional MSNs, these multi-pod structures with altered surface topologies offered higher adhesion efficiency to the biological membrane through enhanced multivalent bio-nano interactions. Moreover, these multi-compartment tetrapod nanocontainers had also shown excellent therapeutic cargo (lysozyme) loading efficiency, resulting in higher performance efficiency, nearly 100% bacteria segregation, and long-term inhibition of over 90%.

Flower-Shaped Packing

In recent times, the fabrication of nature-mimicking designs has garnered enormous interest in expanding the applicability of these innovative siliceous frameworks (Song et al., 2016; Yang et al., 2017). As mentioned earlier, the HMSNs can substantially result in the formation of diverse nature-mimicking designs, including peanut- and rattle-type architectures, by selectively altering the etching agent (Wang et al., 2013). Among various nature-mimicking models, the MSN-based dendritic silica constructs with flower-shaped packing and radial-like direct mesoporous channels offer the advantages of direct and convenient access to the encapsulated guest species due to the presence of a combination of highly tunable small- as well as large-sized pores (Gao et al., 2017; Zheng et al., 2018). These structures can be fabricated by appropriately monitoring the reaction conditions, such as altering of solvent, adding the co-solvent like diethyl ether, structure-directing template, and hydrolysis additives, emulsification of reaction solution, and utilization of catalyst (for instance, triethanolamine), which

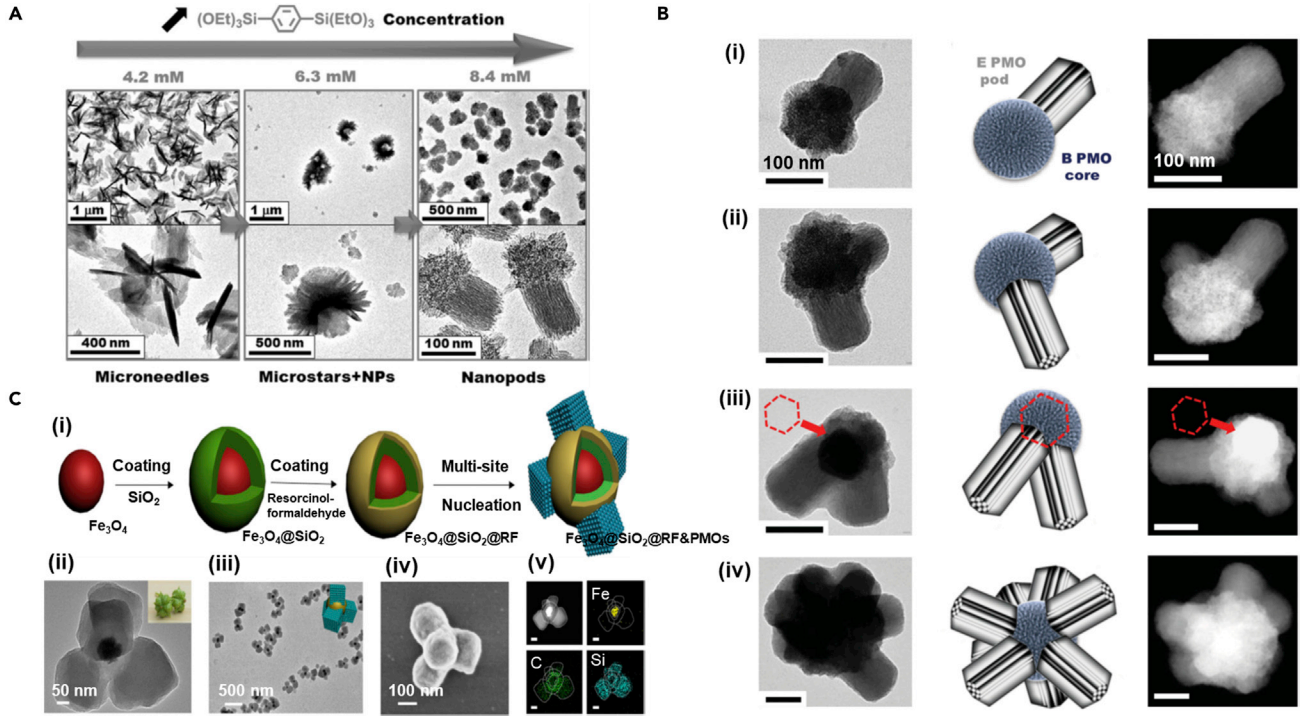

Figure 7. Multi-Podal Architectures

(A) Influence of the 1,4-bis (triethoxysilyl)benzene precursor concentration on the size and morphology of PMO materials, as displayed by TEM micrographs. Reproduced with permission from (Croissant et al., 2016a). Copyright 2016, John Wiley & sons.

(B) TEM images (i-iv) of BE mp-PMO containing one to several pods and corresponding depicted schematic nanoparticle representations and high-resolution scanning transmission electron microscopy (HR-STEM) images. The red hexagons highlight the morphology of the E-PMO pods. Scale bars represent 100 nm. Reproduced with permission from (Croissant et al., 2015a). Copyright 2015, John Wiley & sons.

(C) Synthesis and characterization of Tribulus-like tetrapod nanocomposites. (i) Schematic showing the fabrication process of the tetrapods Fe_3O_4@SiO_2@RF&PMOs nanoparticles based on the surface kinetics-mediated multi-site nucleation strategy. (ii, iii) TEM images at different magnifications, (iv) scanning electron microscope (SEM) image, and (v) element mapping of the Tribulus-like tetrapods Fe_3O_4@SiO_2@RF&PMOs mesoporous nanocomposites. Inset in (ii): a digital photo of Tribulus seeds. Inset in (iii): a 3D structural model of the tetrapods Fe_3O_4@SiO_2@RF&PMOs nanoparticles. Reproduced with permission from (Zhao et al., 2019). Copyright 2019, Nature publishing group.

would substantially influence the reorganization of deposited silica on the pre-MSN core (Gao et al., 2017; Wang et al., 2019a; Zheng et al., 2018). In this vein, the utilization of diethyl ether as a co-solvent had resulted in the multiple morphologies using the biphasic emulsion (O/W) system, in which the wrinkle-shaped architectures were also evident (Du and Qiao, 2015; Wang et al., 2019b). Further efforts using the emulsion system had resulted in the synthesis of silica-based nanospheres with center-radial dendritic frameworks (Du and Qiao, 2015; Wang et al., 2019b). Along this line, Du and coworkers progressed this advancement by adjusting the reaction temperature and stirring speed in the reaction system, resulting in particles (*ca.* 100 to 1100 nm) with center-radial pore sizes (Du et al., 2013, 2015). Such dendritic MSNs have been applied, with a particular interest in the catalysis, synthesis, and medicine. In terms of biomedicine, these center-wide radial porous channels can adsorb the encapsulants, including the large-sized therapeutic molecules such as pDNA and proteins and dyes (Shen et al., 2014; Du and Qiao, 2015; Du et al., 2014; Wang et al., 2019b). In a case, Zhao and coworkers fabricated uniform-sized, discrete 3D dendritic MSNs with tunable center-radial mesochannels (2.8–13 nm) using the heterogeneous oil-water biphase stratification reaction system (Shen et al., 2014). These smart hierarchical architectures offered enhanced loading of bovine β-lactoglobulin, with a loading rate of 62.1 wt %, which could be attributed to the large pore volume of dendritic silica structures. Interestingly, these MSNs presented a long-term sustained release of over 96 hr, in addition to the degradation of MSNs. In another case, Yang and colleagues fabricated multi-shelled dendritic mesoporous organosilica-based hollow spheres toward their utilization as excellent adjuvants, providing superior immunity in cancer immunotherapy (Yang et al., 2017). Similarly, to create an advanced functional platform, Du and colleagues demonstrated not only the gene delivery efficacy but also the tracing by the fluorescence labeling using the dendrimer-like silica nanohybrids with center-radial wide, porous mesochannels (Du et al., 2014).

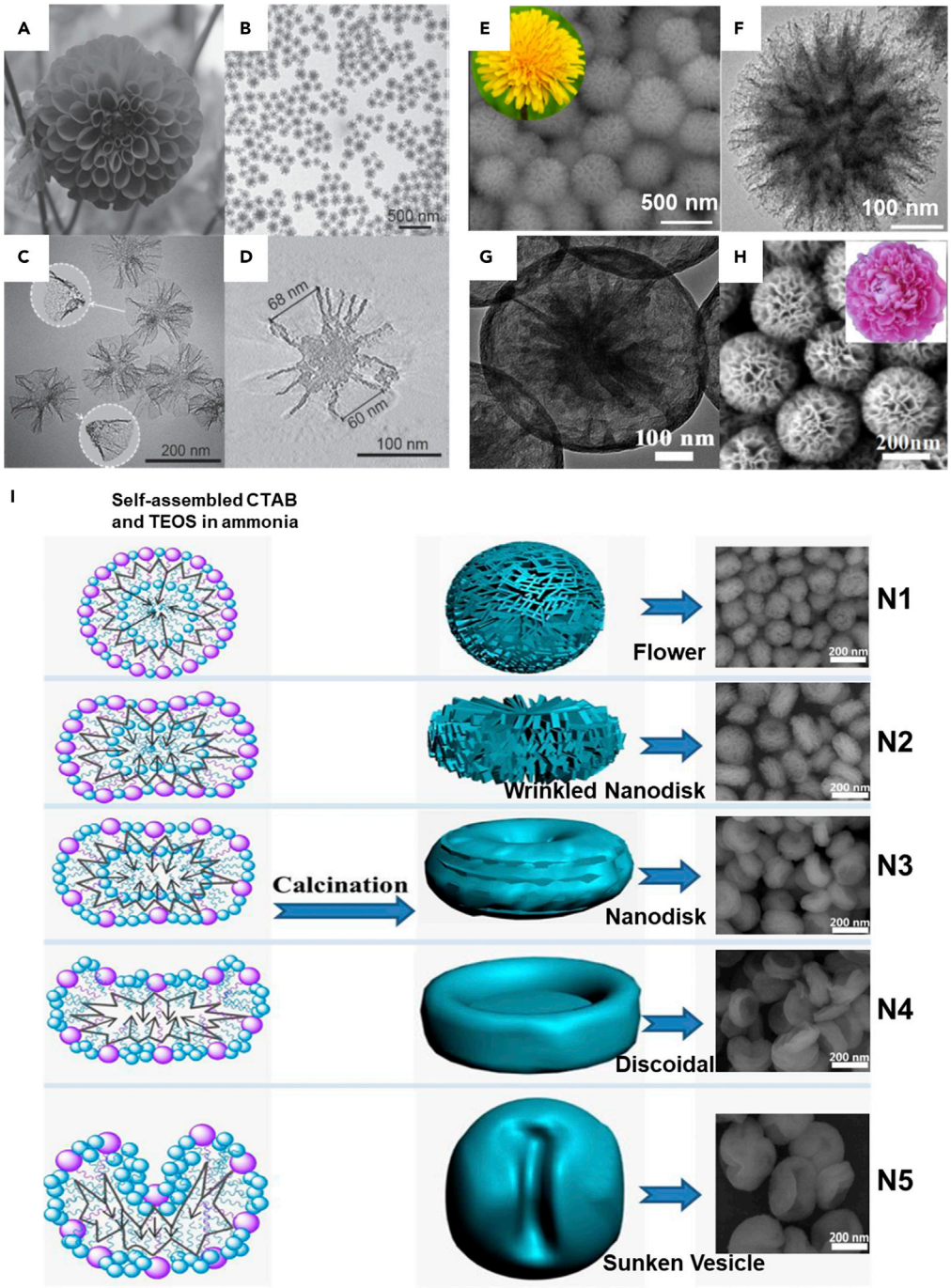

Figure 8. Flower-Shaped Packing of Siliceous Architectures

(A–D) (A) A picture of a dahlia photographed by (C) Xu at Tasmania. TEM images at (B) low magnification, (C) high magnification, and (D) an ET slice of MSNs. Reproduced with permission from (Xu et al., 2015). Copyright 2015, John Wiley & sons.

(E and F) (E) SEM and (F) TEM micrographs of Si O_2 nanoflowers containing elongated spikes, which assembled in a divergent way to form hierarchical dandelion flower-like morphology as shown in the inset of figure E. Reproduced with permission from (Das et al., 2019). Copyright 2019, Elsevier.

(G) TEM images of flower-shaped yolk-shell Si O_2 nanospheres. Reproduced with permission from (Zheng et al., 2018). Copyright 2018, Elsevier.

Figure 8. *Continued*
(H) SEM image of the individual core-shell magnetic organosilica-based nanoflowers with radial wrinkles. Reproduced with permission from (Gao et al., 2017). Copyright 2017, Elsevier.
(I) Illustration representing the synthetic procedure of MSNs with different morphologies. Reproduced with permission from (Chen et al., 2018). Copyright 2018, American Chemical Society.

In the flower-like mesoporous architectures, the arrangement of siloxane moieties or corresponding organosilane often happens to be favorable through a supramolecular self-assembly mechanism (Figures 8A–8D) (Xu et al., 2015). The later formed silica lamellae were organized over the pre-MSN core in the emulsion system with reduced water phase, where the cone-like structures would result in the formation of larger-sized mesopores compared to conventional MSNs. Nevertheless, this approach suffers from a shortcoming of the detachment of the resultant unstable cones during their application, which requires strict optimization of the processing parameters for the fabrication of highly stable architectures. Further, several efforts have been put forward to address the issues through certain advancements such as the addition of hydrolysis additives, for instance, urea, as well as a co-solvent (cyclohexane) and surfactants (cetyl pyridinium bromide) (Das et al., 2019; Gao et al., 2017; Wang et al., 2019a; Zheng et al., 2018). In addition, an external stimulus, for instance, light, can be applied, in which the light-assisted decomposition of urea to ammonium hydroxide resulted in the hydrolysis of added silica precursor. The self-assembly of resultant silicate molecules on CTAB micelles during the condensation reaction would lead to the dandelion flower-like geometrical morphology with elongated spikes and different architectures for carbon dioxide (CO_2) capture (Figures 8E and 8F) (Das et al., 2019). In addition to surfactants, several surface ligands (4-mercaptophenylacetic acid and poly (acrylic acid)) can be used to support in the establishment of multi-nucleation sites over the core materials, such as MNPs, that support in the formation of overlapped silica islands, resulting in the flower-like morphology (Wang et al., 2019a). Utilization of different solvents, such as n-butanol and cyclohexane, leads to the formation of bicontinuous microemulsion at the low surfactant concentrations, referring to the so-called "Winsor III system", resulting in the altered condensation of silica hydrolyzed by urea over the CTAB aggregated on the MNP cores. In such circumstances, several wrinkles produced from the ridges and valleys from the interfaces of bicontinuous microemulsion droplets led to the formation of flower-like structures (Figure 8H) (Gao et al., 2017). Notably, the altered concentrations of the most commonly used, sol-gel-based fabrication catalyst, ammonia that often regulates the hydrolysis and condensation rate of TEOS, could manipulate the overall structure of MSNs ranging from the flower-shaped crystals to nano-sized discoidal and sunken vesicle-like architectures (Figure 8I) (Chen et al., 2018). A steady increase in the concentration of ammonia resulted in the acceleration of hydrolysis and condensation reactions, yielding definite asymmetric structures in diverse shapes. In this regard, the co-solvent pentanol should be highly acknowledgeable in altering the ordered morphology of siliceous structures. Notably, the irregular morphological complexity of flower-like geometry and dendritic structures with wrinkled surfaces and radial spikes yielded better performance over others owing to the large specific surface area.

Inspired by nature, various spiky topological features can also be installed by altering the silica surface towards exhibiting the intriguing surface adhesive properties. In a case, Song and colleagues fabricated silica nanopollens, *i.e.,* silica nanospheres with the extensively rough surface using a facile, one-pot, surfactant-free, cheap, and scalable approach (Song et al., 2016). The synthesis was performed by introducing the formaldehyde resorcinol and TEOS into a typical Stöber synthesis solution, in which the silica was deposited by co-condensation over the resorcinol-formaldehyde core. Further, resorcinol-formaldehyde species penetrating into the shell resulted in inner cavities and spiky surface, resembling the pollen grains. These nanopollens with a rough surface substantially enhanced the adhesion properties of the nanoparticles over other smooth counterparts. In addition, the dense distribution of silica spikes encapsulated with a natural antimicrobial enzyme lysozyme showed the sustained release behavior and substantial antibacterial efficacy towards long-term treatment of bacterial pool in the small intestine. This nature-inspired design provided an ability towards the development of diverse drug delivery carriers exhibiting the adhesion property for enhanced therapeutic efficacy.

Dynamic Modulation

Owing to the highly stiff nature of siloxane bonds, the applicability of MSNs and their eventual fate in the physiological fluids is despicable, which, however, could be addressed by dynamically modulating the siliceous frameworks (Teng et al., 2018). In addition to the final diameter and surface charge, the materials with reversible stiffness and deformable property play a significant role in regulating the communications with

the biological membranes during cellular internalization (Chung et al., 2007). Moreover, such materials with elastic properties and reversible arrangement attributes are of specific interest towards therapy and diagnosis applications over the stiff MSN solids (Chen et al., 2011b). Apart from the offered interactions with biomembranes, these materials can extensively support in achieving the long-term circulation and improved bioavailability in tumors. However, due to their intrinsic rigid siloxane chemical bonds in the hierarchical complex siliceous frameworks, it is highly challenging to achieve the deformability by these conventional MSNs. Nevertheless, incorporating cross-linking organic groups in the thin shells of siliceous frameworks would preferentially be deformable in the physiological fluids. In a case, impregnating the organic groups in the preferentially etched hollow and thin PMO-based siliceous shells resulted in deformable and highly flexible frameworks, in which the shape of MSNs was altered in the physiological environment stumbled with stress. Interestingly, these deformable frameworks significantly enriched the cellular internalization by changing their overall morphology (spherical-to-oval) during the mechanical inner stress by 26-fold over their conventional counterparts (Figure 9A–9C) (Teng et al., 2018). Notably, the comparisons of such materials with other soft constructs such as liposomes and polymer-based constructs could be irrational as the latter composites lack mesostructured characteristics (Teng et al., 2018). Moreover, the deformability of self-assembled noncovalent structure-directing agents would also drive the condensation of silica particles through siloxane linkage formation during their self-assembly (Figure 9D) (Ma et al., 2018). Considering the influence of noncovalent and covalent assembly processes, the surfactant micelle-directed assembly of ultra-small silica-based rings and cage-type structures would result in multi-dimensional materials ranging from 1D cylinders to 2D sheets and 3D helical nanostructures. These structures using such rings as the structural building blocks are now paving their utility towards medicine and other applications. Nonetheless, detailed insights into the pathway complexity are yet remained to be explored.

OUTLOOK

In summary, these innovative mesoporous siliceous frameworks with well-defined pores have offered advantageous physicochemical attributes and morphological, as well as textural properties, which are of particular importance toward diverse biomedical and catalytic applications. However, it is convenient to modify the stable frameworks of MSNs by applying innovative chemistries, to address the inherent challenges of MSNs. In this article, we have provided the state-of-the-art advancements and the intriguing insights on architecting such stable mesoporous siliceous frameworks using various approaches of incorporating inorganic/organic molecular assemblies, resulting in the hetero-nanostructures of irregular-shaped (Janus-type and multi-podal structures) and dynamically-modulated (deformable solids) architectures with high morphological complexity. These innovative composites would substantially facilitate the contributions toward their enhanced applicability through augmented performance, improved biodegradation, enriched physicochemical and morphological attributes along with their structural and colloidal stabilities in the biological environment.

Indeed, much research has been evidenced by the tremendous advancements in MSNs through integrating material science, inorganic chemistry, polymers to precisely control the particle size, orientation, surface, pore size, and MSN frameworks. Although the well-established methods for the synthesis of such MSN-based nanocomposites are available, further steps concerning the optimization of reaction conditions and accurate characterizations to elaborate their performance are required. In addition, cheaper sources of silica, organic groups, and metal salts can support in terms of fabrication towards ease of scale-up and substantial translation. In this vein, we foresee the continuance of innovation in developing simplified and cost-effective preparation methods to explore the versatile, advanced prototypes of MSNs, enabling their batch-to-batch reproducibility towards efficient clinical translation. Moreover, the mesoporous orientation of these innovative architecture MSNs with various assemblies in the frameworks would substantially influence the encapsulation of the guest species. Detailed insights in understanding their orientation are required to dictate their encapsulation and delivery efficiencies in drug delivery applications. We also anticipate that the development of various standard testing systems for evaluating the *in vivo* biosafety will certainly overcome several limitations associated with incomparable assessments from multiple platforms.

Some of these fabricated MSN-based composites, in terms of framework modification, exhibited controlled degradation in the intracellular environment solving the problems of long retention, which, however, requires a detailed understanding in terms of the mechanism involved in the degradation and fate of the resultant products and their influence on the overall elimination pathways from the human

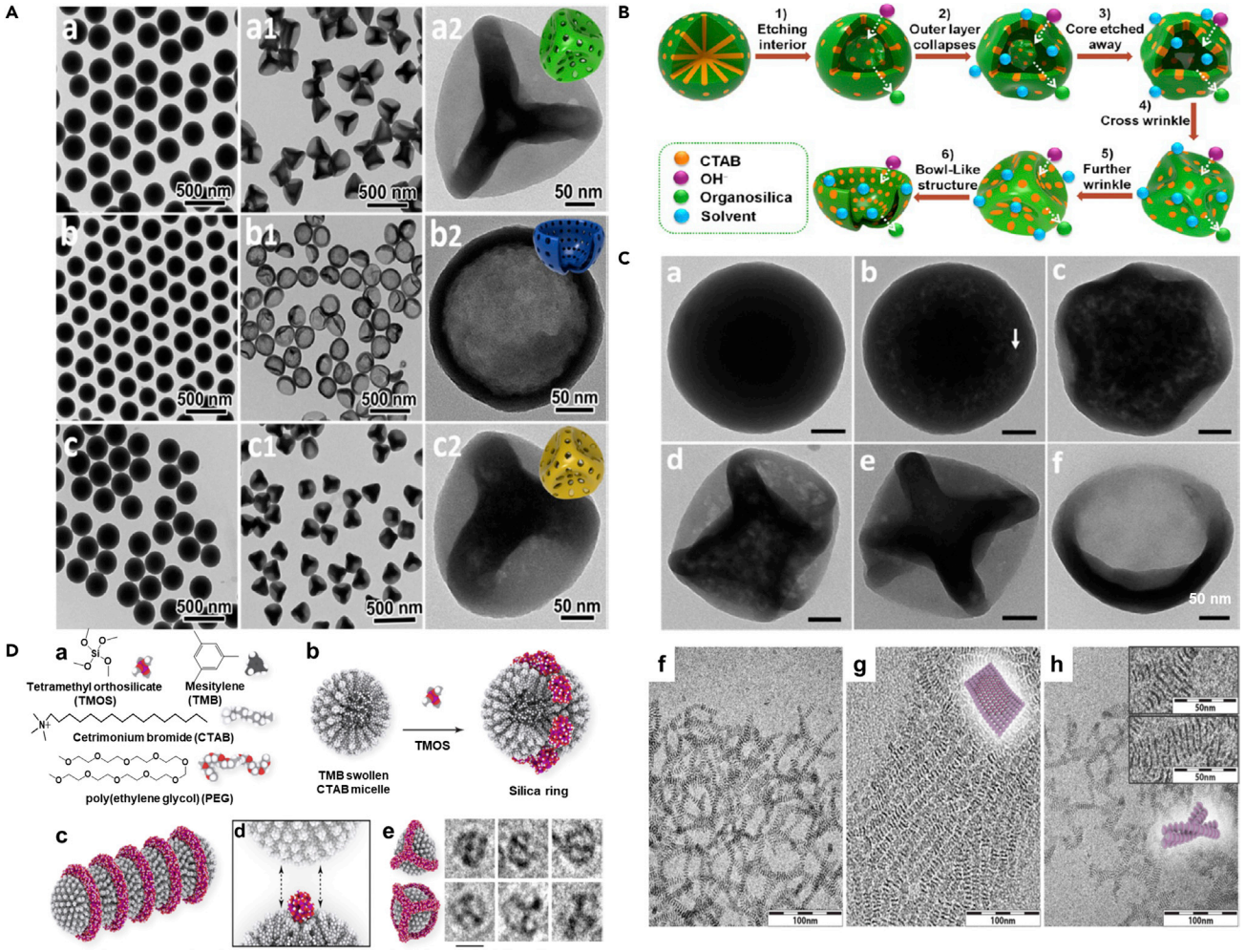

Figure 9. Dynamically Modulated Siliceous Nanoarchitectures

(A–C) (A) TEM images of (a) thioether-, (b) benzene-, and (c) ethane-bridged mesostructured organosilica nanospheres synthesized via a CTAB directed sol-gel process. TEM images of (a1, a2) thioether-, (b1, b2) benzene-, and (c1, c2) ethane-bridged HPMO nanocapsules prepared by etching the corresponding organosilica nanospheres in a mild NaOH solution. Insets in (a2, b2, and c2) are the structural models of the deformed HPMO nanocapsules.

(B) Illustration of the formation mechanism of the deformable HPMO nanocapsules.

(C) TEM images of the thioether-bridged mesostructured organosilica spheres incubated in NaOH aqueous solution (0.48 M) for (a) 1, (b) 3, (c and d) 5, and (e) 20 min, as well as (f) 1 hr. The arrow in (b) indicates the voids. Scale bars represent 50 nm. Reproduced with permission from (Teng et al., 2018). Copyright 2018, American Chemical Society.

(D) Synthesis and characterization of silica rings. (a) Chemical structures. (b) Molecular graphic of the formation of silica rings. (c) A molecular graphic of the worm-like 1D assembly of silica rings. (d) Illustration of micelle surface wrapping around a silica cluster preventing attachment to other micelles (transparent top) due to the strong electrostatic repulsion. (e) Different structures of silica ring with more complex geometries, including rings with one additional arm (top row) and tetrahedral cages (bottom row). Scale bar in the insets: 10 nm. 1D, 2D, and 3D ring assemblies facilitated by PEGs. (f) Cryo-EM image of elongated and segmented 1D ring assemblies obtained upon PEG addition and their substantial transformation to (g) 2D hierarchical arrays of silica rings and (h) 3D assemblies. Reproduced with permission from (Ma et al., 2018). Copyright 2018, American Chemical Society.

body. Moreover, such relevant issues of uncontrolled degradability and the eventual renal clearance of these advanced types of MSNs should also be dynamically controlled. In addition, various long-term toxicity considerations, biosafety evaluations of metal composites encapsulated in the MSNs, and resultant degraded products of disulfide/diselenide-bridged MSN frameworks should be taken into account as they are major biosafety concerns. To achieve this, several steps are required to be taken for monitoring the degradation profile, characterizing the degraded products, requiring detailed mechanistic insights of redox-triggered degradation, and dose optimization to overcome the tolerance threshold due to rapid degradation and *in vivo* clearance. It should be noted that these biosafety relevant issues have not concentrated as much as on the advancements of the MSN fabrications and modification of its frameworks. More

detailed insights are anticipated on the stability, biocompatibility, and efficacy, including the intracellular/extracellular interactions of these modified MSNs toward their utilization for advanced therapeutic modalities.

Using such nanocomposite frameworks of MSNs in combination with various metals toward advanced therapeutic modalities, the catalytic nanomedicine is developed and applied for achieving the augmented therapeutic effects. Considering these aspects, versatile materials are expected to be designed, which, however, on the grounds of promising therapeutic and compatibility abilities. Although such versatile materials are developed, several questions based on their clinical approval remain unanswered as the animal studies fail to replicate the translation procedures in humans due to problems in biodistribution and biosafety issues. Possibly, the convenient way to address these aspects is to put the design of MSN-based nanocomposites as versatile and simple, considering the factors of cost-effective synthesis, high payload, targeting ability, biodegradability, biocompatibility, and rapid clearance, which are being expected by the regulatory authorities and industries for biosafety.

Together, we believe that the outcomes of potential advancements through close collaborations of material scientists and biologists will undoubtedly facilitate the promising routes of alleviating or overcoming limitations on therapeutic results and profoundly highlight the significant contributions in multidisciplinary fields. In the end, the combination of versatility with innovative chemistries and complementary strategies that will facilitate their exploration towards innovative applications of this class will continue to emerge.

ACKNOWLEDGMENTS

The authors sincerely acknowledge financial support from the National Natural Science Foundation of China (NSFC, 31800794, U1605225, and 81971734), Natural Science Foundation of Fujian Province (2019J01076), the support by the Fundamental Research Funds for the Central Universities (ZQN-713), Funds for Foreign Experts from Ministry of Science and Technology, China (G20190013023), and Program for Innovative Research Team in Science and Technology in Fujian Province University. We sincerely thank Ya Hui Han and Lokesh Kumar Mende for assisting us in the figure illustrations and valuable discussions.

AUTHOR CONTRIBUTIONS

R.K.K proposed the outline and compiled the review manuscript. S.B. W and A.Z. C. revised the manuscript with some meticulous discussions.

REFERENCES

Abbaraju, P.L., Meka, A.K., Song, H., Yang, Y., Jambhrunkar, M., Zhang, J., Xu, C., Yu, M., and Yu, C. (2017). Asymmetric silica nanoparticles with tunable head–tail structures enhance hemocompatibility and maturation of immune cells. J. Am. Chem. Soc. *139*, 6321–6328.

An, N., Lin, H., Yang, C., Zhang, T., Tong, R., Chen, Y., and Qu, F. (2016). Gated magnetic mesoporous silica nanoparticles for intracellular enzyme-triggered drug delivery. Mater. Sci. Eng. C *69*, 292–300.

Argyo, C., Weiss, V., Bräuchle, C., and Bein, T. (2014). Multifunctional mesoporous silica nanoparticles as a universal platform for drug delivery. Chem. Mater. *26*, 435–451.

Asefa, T., MacLachlan, M.J., Coombs, N., and Ozin, G.A. (1999). Periodic mesoporous organosilicas with organic groups inside the channel walls. Nature *402*, 867–871.

Aspromonte, S.G., Sastre, Á., Boix, A.V., Cocero, M.J., and Alonso, E. (2012). Cobalt oxide nanoparticles on mesoporous MCM-41 and Al-MCM-41 by supercritical CO2 deposition. Microporous Mesoporous Mater. *148*, 53–61.

Beck, J.S., Vartuli, J.C., Roth, W.J., Leonowicz, M.E., Kresge, C.T., Schmitt, K.D., Chu, C.T.W., Olson, D.H., Sheppard, E.W., McCullen, S.B., et al. (1992). A new family of mesoporous molecular sieves prepared with liquid crystal templates. J. Am. Chem. Soc. *114*, 10834–10843.

Byoun, W., Jung, S., Tran, N.M., and Yoo, H. (2018). Synthesis and application of dendritic fibrous nanosilica/gold hybrid nanomaterials. ChemistryOpen *7*, 349–355.

Cai, Q., Luo, Z.-S., Pang, W.-Q., Fan, Y.-W., Chen, X.-H., and Cui, F.-Z. (2001). Dilute solution routes to various controllable morphologies of MCM-41 silica with a basic medium. Chem. Mater. *13*, 258–263.

Cesteros, Y., and Haller, G.L. (2001). Several factors affecting Al-MCM-41 synthesis. Microporous Mesoporous Mater. *43*, 171–179.

Chen, C.-Y., Li, H.-X., and Davis, M.E. (1993). Studies on mesoporous materials: I. Synthesis and characterization of MCM-41. Microporous Mater. *2*, 17–26.

Chen, G., Xie, Y., Peltier, R., Lei, H., Wang, P., Chen, J., Hu, Y., Wang, F., Yao, X., and Sun, H. (2016). Peptide-decorated gold nanoparticles as functional nano-capping agent of mesoporous silica container for targeting drug delivery. ACS Appl. Mater. Inter. *8*, 11204–11209.

Chen, J., Sheng, Y., Song, Y., Chang, M., Zhang, X., Cui, L., Meng, D., Zhu, H., Shi, Z., and Zou, H. (2018). Multimorphology mesoporous silica nanoparticles for dye adsorption and multicolor luminescence applications. ACS Sustain. Chem. Eng. *6*, 3533–3545.

Chen, L., Di, J., Cao, C., Zhao, Y., Ma, Y., Luo, J., Wen, Y., Song, W., Song, Y., and Jiang, L. (2011a). A pH-driven DNA nanoswitch for responsive controlled release. Chem. Commun. *47*, 2850–2852.

Chen, P.-J., Hu, S.-H., Hsiao, C.-S., Chen, Y.-Y., Liu, D.-M., and Chen, S.-Y. (2011b). Multifunctional magnetically removable nanogated lids of Fe3O4-capped mesoporous silica nanoparticles for intracellular controlled release and MR imaging. J. Mater. Chem. *21*, 2535–2543.

Chen, Y., Chen, H., and Shi, J. (2013). In vivo bio-safety evaluations and diagnostic/therapeutic applications of chemically designed mesoporous silica nanoparticles. Adv. Mater. *25*, 3144–3176.

Chen, Y., Meng, Q., Wu, M., Wang, S., Xu, P., Chen, H., Li, Y., Zhang, L., Wang, L., and Shi, J. (2014). Hollow mesoporous organosilica nanoparticles: a generic intelligent framework-hybridization approach for biomedicine. J. Am. Chem. Soc. *136*, 16326–16334.

Cho, E.-B., Kim, D., Gorka, J., and Jaroniec, M. (2009). Three-dimensional cubic (Im3m) periodic mesoporous organosilicas with benzene- and thiophene-bridging groups. J. Mater. Chem. *19*, 2076–2081.

Chung, T.H., Wu, S.H., Yao, M., Lu, C.W., Lin, Y.S., Hung, Y., Mou, C.Y., Chen, Y.C., and Huang, D.M. (2007). The effect of surface charge on the uptake and biological function of mesoporous silica nanoparticles in 3T3-L1 cells and human mesenchymal stem cells. Biomaterials *28*, 2959–2966.

Corma, A., Fornes, V., Navarro, M.T., and Perezpariente, J. (1994). Acidity and stability of MCM-41 crystalline aluminosilicates. J. Catal. *148*, 569–574.

Croissant, J., Cattoën, X., Man, M.W.C., Gallud, A., Raehm, L., Trens, P., Maynadier, M., and Durand, J.-O. (2014a). Biodegradable ethylene-bis (Propyl)Disulfide-based periodic mesoporous organosilica nanorods and nanospheres for efficient in-vitro drug delivery. Adv. Mater. *26*, 6174–6180.

Croissant, J., Cattoën, X., Wong Chi Man, M., Dieudonné, P., Charnay, C., Raehm, L., and Durand, J.-O. (2015a). One-pot construction of multipodal hybrid periodic mesoporous organosilica nanoparticles with crystal-like architectures. Adv. Mater. *27*, 145–149.

Croissant, J., Salles, D., Maynadier, M., Mongin, O., Hugues, V., Blanchard-Desce, M., Cattoën, X., Wong Chi Man, M., Gallud, A., Garcia, M., et al. (2014b). Mixed periodic mesoporous organosilica nanoparticles and core–shell systems, application to in vitro two-photon imaging, therapy, and drug delivery. Chem. Mater. *26*, 7214–7220.

Croissant, J.G., Cattoen, X., Wong, M.C., Durand, J.O., and Khashab, N.M. (2015b). Syntheses and applications of periodic mesoporous organosilica nanoparticles. Nanoscale *7*, 20318–20334.

Croissant, J.G., Fatieiev, Y., Almalik, A., and Khashab, N.M. (2018). Mesoporous silica and organosilica nanoparticles: physical chemistry, biosafety, delivery strategies, and biomedical applications. Adv. Healthc. Mater *7*, 1700831.

Croissant, J.G., Fatieiev, Y., Omar, H., Anjum, D.H., Gurinov, A., Lu, J., Tamanoi, F., Zink, J.I., and Khashab, N.M. (2016a). Periodic mesoporous organosilica nanoparticles with controlled morphologies and high drug/dye loadings for multicargo delivery in cancer cells. Chem. Eur. J. *22*, 9607–9615.

Croissant, J.G., Zhang, D., Alsaiari, S., Lu, J., Deng, L., Tamanoi, F., AlMalik, A.M., Zink, J.I., and Khashab, N.M. (2016b). Protein-gold clusters-capped mesoporous silica nanoparticles for high drug loading, autonomous gemcitabine/doxorubicin co-delivery, and in-vivo tumor imaging. J. Control. Release *229*, 183–191.

Das, S., Samanta, A., and Jana, S. (2019). Light-driven synthesis of uniform dandelion-like mesoporous silica nanoflowers with tunable surface area for carbon dioxide uptake. Chem. Eng. J. *374*, 1118–1126.

Dinker, M.K., and Kulkarni, P.S. (2016). Insight into the PEG-linked bis-imidazolium bridged framework of mesoporous organosilicas as ion exchangers. Microporous Mesoporous Mater. *230*, 145–153.

Du, X., Kleitz, F., Li, X., Huang, H., Zhang, X., and Qiao, S.-Z. (2018a). Disulfide-bridged organosilica frameworks: designed, synthesis, redox-triggered biodegradation, and nanobiomedical applications. Adv. Funct. Mater. *28*, 1707325.

Du, X., Li, W., Shi, B., Su, L., Li, X., Huang, H., Wen, Y., and Zhang, X. (2018b). Facile synthesis of mesoporous organosilica nanobowls with bridged silsesquioxane framework by one-pot growth and dissolution mechanism. J. Colloid Interf. Sci. *528*, 379–388.

Du, X., Li, X., Huang, H., He, J., and Zhang, X. (2015). Dendrimer-like hybrid particles with tunable hierarchical pores. Nanoscale *7*, 6173–6184.

Du, X., Li, X., Xiong, L., Zhang, X., Kleitz, F., and Qiao, S.Z. (2016). Mesoporous silica nanoparticles with organo-bridged silsesquioxane framework as innovative platforms for bioimaging and therapeutic agent delivery. Biomaterials *91*, 90–127.

Du, X., and Qiao, S.Z. (2015). Dendritic silica particles with center-radial pore channels: promising platforms for catalysis and biomedical applications. Small *11*, 392–413.

Du, X., Shi, B., Liang, J., Bi, J., Dai, S., and Qiao, S.Z. (2013). Developing functionalized dendrimer-like silica nanoparticles with hierarchical pores as advanced delivery nanocarriers. Adv. Mater. *25*, 5981–5985.

Du, X., Shi, B., Tang, Y., Dai, S., and Qiao, S.Z. (2014). Label-free dendrimer-like silica nanohybrids for traceable and controlled gene delivery. Biomaterials *35*, 5580–5590.

Eimer, G.A., Pierella, L.B., Monti, G.A., and Anunziata, O.A. (2002). Synthesis and characterization of Al-MCM-41 and Al-MCM-48 mesoporous materials. Catal. Lett. *78*, 65–75.

Fang, J., Zhang, L., Li, J., Lu, L., Ma, C., Cheng, S., Li, Z., Xiong, Q., and You, H. (2018). A general soft-enveloping strategy in the templating synthesis of mesoporous metal nanostructures. Nat. Commun. *9*, 521.

Fatieiev, Y., Croissant, J.G., Alamoudi, K., and Khashab, N.M. (2017). Cellular internalization and biocompatibility of periodic mesoporous organosilica nanoparticles with tunable morphologies: from nanospheres to nanowires. ChemPlusChem *82*, 631–637.

Fowler, C.E., Khushalani, D., Lebeau, B., and Mann, S. (2001). Nanoscale materials with mesostructured interiors. Adv. Mater. *13*, 649–652.

Gao, J., Kong, W., Zhou, L., He, Y., Ma, L., Wang, Y., Yin, L., and Jiang, Y. (2017). Monodisperse core-shell magnetic organosilica nanoflowers with radial wrinkle for lipase immobilization. Chem. Eng. J. *309*, 70–79.

Geng, H., Chen, W., Xu, Z.P., Qian, G., An, J., and Zhang, H. (2017). Shape-controlled hollow mesoporous silica nanoparticles with multifunctional capping for in vitro cancer treatment. Chem. Eur. J. *23*, 10878–10885.

Grosch, L., Lee, Y.J., Hoffmann, F., and Froba, M. (2015). Light-harvesting three-chromophore systems based on biphenyl-bridged periodic mesoporous organosilica. Chem. Eur. J. *21*, 331–346.

Grün, M., Lauer, I., and Unger, K.K. (1997). The synthesis of micrometer- and submicrometer-size spheres of ordered mesoporous oxide MCM-41. Adv. Mater. *9*, 254–257.

Guan, B., Cui, Y., Ren, Z., Qiao, Z.-a., Wang, L., Liu, Y., and Huo, Q. (2012). Highly ordered periodic mesoporous organosilica nanoparticles with controllable pore structures. Nanoscale *4*, 6588–6596.

Hadipour Moghaddam, S.P., Yazdimamaghani, M., and Ghandehari, H. (2018). Glutathione-sensitive hollow mesoporous silica nanoparticles for controlled drug delivery. J. Control. Release *282*, 62–75.

Han, Y., and Ying, J.Y. (2005). Generalized fluorocarbon-surfactant-mediated synthesis of nanoparticles with various mesoporous structures. Angew. Chem. Int. Ed. *44*, 288–292.

He, Q., Zhang, J., Shi, J., Zhu, Z., Zhang, L., Bu, W., Guo, L., and Chen, Y. (2010). The effect of PEGylation of mesoporous silica nanoparticles on nonspecific binding of serum proteins and cellular responses. Biomaterials *31*, 1085–1092.

He, Q., Zhang, Z., Gao, F., Li, Y., and Shi, J. (2011). In vivo biodistribution and urinary excretion of mesoporous silica nanoparticles: effects of particle size and PEGylation. Small *7*, 271–280.

Hu, J., Chen, M., Fang, X., and Wu, L. (2011). Fabrication and application of inorganic hollow spheres. Chem. Soc. Rev. *40*, 5472–5491.

Huang, P., Chen, Y., Lin, H., Yu, L., Zhang, L., Wang, L., Zhu, Y., and Shi, J. (2017). Molecularly organic/inorganic hybrid hollow mesoporous organosilica nanocapsules with tumor-specific biodegradability and enhanced chemotherapeutic functionality. Biomaterials *125*, 23–37.

Hudson, S.P., Padera, R.F., Langer, R., and Kohane, D.S. (2008). The biocompatibility of mesoporous silicates. Biomaterials *29*, 4045–4055.

Huh, S., Wiench, J.W., Trewyn, B.G., Song, S., Pruski, M., and Lin, V.S. (2003). Tuning of particle morphology and pore properties in mesoporous silicas with multiple organic functional groups. Chem. Commun. *9*, 2364–2365.

Huo, C., Ouyang, J., and Yang, H. (2014). CuO nanoparticles encapsulated inside Al-MCM-41 mesoporous materials via direct synthetic route. Sci. Rep. *4*, 3682.

Inagaki, S., Guan, S., Fukushima, Y., Ohsuna, T., and Terasaki, O. (1999). Novel mesoporous materials with a uniform distribution of organic

groups and inorganic oxide in their frameworks. J. Am. Chem. Soc. *121*, 9611–9614.

Jhaveri, A., and Torchilin, V. (2016). Intracellular delivery of nanocarriers and targeting to subcellular organelles. Exp. Opin. Drug Deliv. *13*, 49–70.

Kankala, R.K., Han, Y.-H., Na, J., Lee, C.-H., Sun, Z., Wang, S.-B., Kimura, T., Ok, Y.S., Yamauchi, Y., Chen, A.-Z., et al. (2020a). Nanoarchitectured structure and surface biofunctionality of mesoporous silica nanoparticles. Adv. Mater. *32*, 1907035.

Kankala, R.K., Kuthati, Y., Liu, C.-L., Mou, C.-Y., and Lee, C.-H. (2015). Killing cancer cells by delivering a nanoreactor for inhibition of catalase and catalytically enhancing intracellular levels of ROS. RSC Adv. *5*, 86072–86081.

Kankala, R.K., Lin, W.Z., and Lee, C.H. (2020b). Combating antibiotic resistance through the synergistic effects of mesoporous silica-based hierarchical nanocomposites. Nanomaterials (Basel, Switzerland) *10*, 597.

Kankala, R.K., Liu, C.-G., Chen, A.-Z., Wang, S.-B., Xu, P.-Y., Mende, L.K., Liu, C.-L., Lee, C.-H., and Hu, Y.-F. (2017). Overcoming multidrug resistance through the synergistic effects of hierarchical pH-sensitive, ROS-generating nanoreactors. ACS Biomater. Sci. Eng. *3*, 2431.

Kankala, R.K., Liu, C.-G., Yang, D.-Y., Wang, S.-B., and Chen, A.-Z. (2020c). Ultrasmall platinum nanoparticles enable deep tumor penetration and synergistic therapeutic abilities through free radical species-assisted catalysis to combat cancer multidrug resistance. Chem. Eng. J. *383*, 123138.

Kankala, R.K., Zhang, H., Liu, C.-G., Kanubaddi, K.R., Lee, C.-H., Wang, S.-B., Cui, W., Santos, H.A., Lin, K., and Chen, A.-Z. (2019). Metal species–encapsulated mesoporous silica nanoparticles: current advancements and latest breakthroughs. Adv. Funct. Mater. *29*, 1902652.

Karimi, M., Sahandi Zangabad, P., Baghaee-Ravari, S., Ghazadeh, M., Mirshekari, H., and Hamblin, M.R. (2017). Smart nanostructures for cargo delivery: uncaging and activating by light. J. Am. Chem. Soc. *139*, 4584–4610.

Kim, J.H., Fang, B., Song, M.Y., and Yu, J.-S. (2012). Topological transformation of thioether-bridged organosilicas into nanostructured functional materials. Chem. Mater. *24*, 2256–2264.

Kolodziejski, W., Corma, A., Navarro, M.-T., and Pérez-Pariente, J. (1993). Solid-state NMR study of ordered mesoporous aluminosilicate MCM-41 synthesized on a liquid-crystal template. Solid State Nucl. Magn. Reson. *2*, 253–259.

Kresge, C.T., Leonowicz, M.E., Roth, W.J., Vartuli, J.C., and Beck, J.S. (1992). Ordered mesoporous molecular sieves synthesized by a liquid-crystal template mechanism. Nature *359*, 710–712.

Kuthati, Y., Kankala, R.K., Busa, P., Lin, S.-X., Deng, J.-P., Mou, C.-Y., and Lee, C.-H. (2017). Phototherapeutic spectrum expansion through synergistic effect of mesoporous silica trio-nanohybrids against antibiotic-resistant gram-negative bacterium. J. Photochem. Photobiol. B *169*, 124–133.

Lai, C.-Y., Trewyn, B.G., Jeftinija, D.M., Jeftinija, K., Xu, S., Jeftinija, S., and Lin, V.S.Y. (2003). A mesoporous silica nanosphere-based carrier system with chemically removable CdS nanoparticle caps for stimuli-responsive controlled release of neurotransmitters and drug molecules. J. Am. Chem. Soc. *125*, 4451–4459.

Landau, M.V., Dafa, E., Kaliya, M.L., Sen, T., and Herskowitz, M. (2001). Mesoporous alumina catalytic material prepared by grafting wide-pore MCM-41 with an alumina multilayer. Microporous Mesoporous Mater. *49*, 65–81.

Lee, C.-H., Lin, T.-S., and Mou, C.-Y. (2009). Mesoporous materials for encapsulating enzymes. Nano Today *4*, 165–179.

Lee, J.E., Lee, N., Kim, T., Kim, J., and Hyeon, T. (2011). Multifunctional mesoporous silica nanocomposite nanoparticles for theranostic applications. Acc. Chem. Res. *44*, 893–902.

Li, X., Zhou, L., Wei, Y., El-Toni, A.M., Zhang, F., and Zhao, D. (2014). Anisotropic growth-induced synthesis of dual-compartment Janus mesoporous silica nanoparticles for bimodal triggered drugs delivery. J. Am. Chem. Soc. *136*, 15086–15092.

Li, Y., Li, N., Pan, W., Yu, Z., Yang, L., and Tang, B. (2017). Hollow mesoporous silica nanoparticles with tunable structures for controlled drug delivery. ACS Appl. Mater. Inter. *9*, 2123–2129.

Lin, Y.-S., Tsai, C.-P., Huang, H.-Y., Kuo, C.-T., Hung, Y., Huang, D.-M., Chen, Y.-C., and Mou, C.-Y. (2005). Well-ordered mesoporous silica nanoparticles as cell markers. Chem. Mater. *17*, 4570–4573.

Liong, M., Lu, J., Kovochich, M., Xia, T., Ruehm, S.G., Nel, A.E., Tamanoi, F., and Zink, J.I. (2008). Multifunctional inorganic nanoparticles for imaging, targeting, and drug delivery. ACS Nano *2*, 889–896.

Liu, C.-G., Han, Y.-H., Kankala, R.K., Wang, S.-B., and Chen, A.-Z. (2020). Subcellular performance of nanoparticles in cancer therapy. Int. J. Nanomedicine *15*, 675–704.

Liu, C.-G., Han, Y.-H., Zhang, J.-T., Kankala, R.K., Wang, S.-B., and Chen, A.-Z. (2019). Rerouting engineered metal-dependent shapes of mesoporous silica nanocontainers to biodegradable Janus-type (sphero-ellipsoid) nanoreactors for chemodynamic therapy. Chem. Eng. J. *370*, 1188–1199.

Lou, X.W., Archer, L.A., and Yang, Z. (2008). Hollow micro-/nanostructures: synthesis and applications. Adv. Mater. *20*, 3987–4019.

Ma, K., Spoth, K.A., Cong, Y., Zhang, D., Aubert, T., Turker, M.Z., Kourkoutis, L.F., Mendes, E., and Wiesner, U. (2018). Early formation pathways of surfactant micelle directed ultrasmall silica ring and cage structures. J. Am. Chem. Soc. *140*, 17343–17348.

Ma, X., Hahn, K., and Sanchez, S. (2015). Catalytic mesoporous Janus nanomotors for active cargo delivery. J. Am. Chem. Soc. *137*, 4976–4979.

Maegawa, Y., and Inagaki, S. (2015). Iridium-bipyridine periodic mesoporous organosilica catalyzed direct C-H borylation using a pinacolborane. Dalton Trans. *44*, 13007–13016.

Maggini, L., Cabrera, I., Ruiz-Carretero, A., Prasetyanto, E.A., Robinet, E., and De Cola, L. (2016). Breakable mesoporous silica nanoparticles for targeted drug delivery. Nanoscale *8*, 7240–7247.

Mekaru, H., Lu, J., and Tamanoi, F. (2015). Development of mesoporous silica-based nanoparticles with controlled release capability for cancer therapy. Adv. Drug Deliv. Rev. *95*, 40–49.

Melde, B.J., Holland, B.T., Blanford, C.F., and Stein, A. (1999). Mesoporous sieves with unified hybrid inorganic/organic frameworks. Chem. Mater. *11*, 3302–3308.

Mizoshita, N., and Inagaki, S. (2015). Periodic mesoporous organosilica with molecular-scale ordering self-assembled by hydrogen bonds. Angew. Chem. Int. Ed. *54*, 11999–12003.

Monnier, A., Schüth, F., Huo, Q., Kumar, D., Margolese, D., Maxwell, R.S., Stucky, G.D., Krishnamurty, M., Petroff, P., Firouzi, A., et al. (1993). Cooperative formation of inorganic-organic interfaces in the synthesis of silicate mesostructures. Science *261*, 1299–1303.

Niedermayer, S., Weiss, V., Herrmann, A., Schmidt, A., Datz, S., Muller, K., Wagner, E., Bein, T., and Brauchle, C. (2015). Multifunctional polymer-capped mesoporous silica nanoparticles for pH-responsive targeted drug delivery. Nanoscale *7*, 7953–7964.

Niu, D., Ma, Z., Li, Y., and Shi, J. (2010). Synthesis of core-shell structured dual-mesoporous silica spheres with tunable pore size and controllable shell thickness. J. Am. Chem. Soc. *132*, 15144–15147.

Niu, K., Liang, L., Gu, Y., Ke, L., Duan, F., and Chen, M. (2011). Fabrication and photoluminescent properties of ZnO/mesoporous silica composites templated by a chelating surfactant. Langmuir *27*, 13820–13827.

Parvulescu, V., and Su, B.L. (2001). Iron, cobalt or nickel substituted MCM-41 molecular sieves for oxidation of hydrocarbons. Catal. Today *69*, 315–322.

Popat, A., Hartono, S.B., Stahr, F., Liu, J., Qiao, S.Z., and Lu, G.Q. (2011). Mesoporous silica nanoparticles for bioadsorption, enzyme immobilisation, and delivery carriers. Nanoscale *3*, 2801–2818.

Prasetyanto, E.A., Bertucci, A., Septiadi, D., Corradini, R., Castro-Hartmann, P., and DeCola, L. (2016). Breakable hybrid organosilica nanocapsules for protein delivery. Angew. Chem. Int. Ed. *55*, 3323–3327.

Quesada, M., Muniesa, C., and Botella, P. (2013). Hybrid PLGA-organosilica nanoparticles with redox-sensitive molecular gates. Chem. Mater. *25*, 2597–2602.

Riehemann, K., Schneider, S.W., Luger, T.A., Godin, B., Ferrari, M., and Fuchs, H. (2009). Nanomedicine–challenge and perspectives. Angew. Chem. Int. Ed. *48*, 872–897.

Rosenholm, J.M., Meinander, A., Peuhu, E., Niemi, R., Eriksson, J.E., Sahlgren, C., and Lindén, M. (2009). Targeting of porous hybrid silica

nanoparticles to cancer cells. ACS Nano *3*, 197–206.

Rosenholm, J.M., Sahlgren, C., and Lindén, M. (2010). Towards multifunctional, targeted drug delivery systems using mesoporous silica nanoparticles – opportunities & challenges. Nanoscale *2*, 1870–1883.

Rosenholm, J.M., Zhang, J., Linden, M., and Sahlgren, C. (2016). Mesoporous silica nanoparticles in tissue engineering – a perspective. Nanomedicine *11*, 391–402.

Ryoo, R., Ko, C.H., and Howe, R.F. (1997). Imaging the distribution of framework aluminum in mesoporous molecular sieve MCM-41. Chem. Mater. *9*, 1607–1613.

Sánchez, A., Díez, P., Martínez-Ruíz, P., Villalonga, R., and Pingarrón, J.M. (2013). Janus Au-mesoporous silica nanoparticles as electrochemical biorecognition-signaling system. Electrochem. Commun. *30*, 51–54.

Sayari, A., and Wang, W. (2005). Molecularly ordered nanoporous organosilicates prepared with and without surfactants. J. Am. Chem. Soc. *127*, 12194–12195.

Shao, D., Li, M., Wang, Z., Zheng, X., Lao, Y.-H., Chang, Z., Zhang, F., Lu, M., Yue, J., Hu, H., et al. (2018). Bioinspired diselenide-bridged mesoporous silica nanoparticles for dual-responsive protein delivery. Adv. Mater. *30*, 1801198.

Shao, D., Zhang, X., Liu, W., Zhang, F., Zheng, X., Qiao, P., Li, J., Dong, W.F., and Chen, L. (2016). Janus silver-mesoporous silica nanocarriers for SERS traceable and pH-sensitive drug delivery in cancer therapy. ACS Appl. Mater. Inter. *8*, 4303–4308.

Shen, D., Yang, J., Li, X., Zhou, L., Zhang, R., Li, W., Chen, L., Wang, R., Zhang, F., and Zhao, D. (2014). Biphase stratification approach to three-dimensional dendritic biodegradable mesoporous silica nanospheres. Nano Lett. *14*, 923–932.

Slowing, I.I., Vivero-Escoto, J.L., Wu, C.-W., and Lin, V.S.Y. (2008). Mesoporous silica nanoparticles as controlled release drug delivery and gene transfection carriers. Adv. Drug Deliv. Rev. *60*, 1278–1288.

Song, H., Ahmad Nor, Y., Yu, M., Yang, Y., Zhang, J., Zhang, H., Xu, C., Mitter, N., and Yu, C. (2016). Silica nanopollens enhance adhesion for long-term bacterial inhibition. J. Am. Chem. Soc. *138*, 6455–6462.

Sun, Y., and Xia, Y. (2002). Shape-controlled synthesis of gold and silver nanoparticles. Science *298*, 2176–2179.

Suteewong, T., Sai, H., Hovden, R., Muller, D., Bradbury, M.S., Gruner, S.M., and Wiesner, U. (2013). Multicompartment mesoporous silica nanoparticles with branched shapes: an epitaxial growth mechanism. Science *340*, 337–341.

Tao, Z. (2014). Mesoporous silica-based nanodevices for biological applications. RSC Adv. *4*, 18961–18980.

Tarn, D., Ashley, C.E., Xue, M., Carnes, E.C., Zink, J.I., and Brinker, C.J. (2013). Mesoporous silica nanoparticle nanocarriers: biofunctionality and biocompatibility. Acc. Chem. Res. *46*, 792–801.

Teng, Z., Li, W., Tang, Y., Elzatahry, A., Lu, G., and Zhao, D. (2019). Mesoporous organosilica hollow nanoparticles: synthesis and applications. Adv. Mater. *31*, 1707612.

Teng, Z., Su, X., Lee, B., Huang, C., Liu, Y., Wang, S., Wu, J., Xu, P., Sun, J., Shen, D., et al. (2014). Yolk–shell structured mesoporous nanoparticles with thioether-bridged organosilica frameworks. Chem. Mater. *26*, 5980–5987.

Teng, Z., Su, X., Zheng, Y., Zhang, J., Liu, Y., Wang, S., Wu, J., Chen, G., Wang, J., Zhao, D., et al. (2015). A facile multi-interface transformation approach to monodisperse multiple-shelled periodic mesoporous organosilica hollow spheres. J. Am. Chem. Soc. *137*, 7935–7944.

Teng, Z., Wang, C., Tang, Y., Li, W., Bao, L., Zhang, X., Su, X., Zhang, F., Zhang, J., Wang, S., et al. (2018). Deformable hollow periodic mesoporous organosilica nanocapsules for significantly improved cellular uptake. J. Am. Chem. Soc. *140*, 1385–1393.

Tian, W., Su, Y., Tian, Y., Wang, S., Su, X., Liu, Y., Zhang, Y., Tang, Y., Ni, Q., Liu, W., et al. (2017). Periodic mesoporous organosilica coated prussian blue for MR/PA dual-modal imaging-guided photothermal-chemotherapy of Triple negative breast cancer. Adv. Sci. *4*, 1600356.

Trewyn, B.G., Slowing, I.I., Giri, S., Chen, H.-T., and Lin, V.S.Y. (2007). Synthesis and functionalization of a mesoporous silica nanoparticle based on the sol–gel process and applications in controlled release. Acc. Chem. Res. *40*, 846–853.

Ujiie, H., Shimojima, A., and Kuroda, K. (2015). Synthesis of colloidal Janus nanoparticles by asymmetric capping of mesoporous silica with phenylsilsesquioxane. Chem. Commun. *51*, 3211–3214.

Urata, C., Yamada, H., Wakabayashi, R., Aoyama, Y., Hirosawa, S., Arai, S., Takeoka, S., Yamauchi, Y., and Kuroda, K. (2011). Aqueous colloidal mesoporous nanoparticles with ethenylene-bridged silsesquioxane frameworks. J. Am. Chem. Soc. *133*, 8102–8105.

Villalonga, R., Diez, P., Sanchez, A., Aznar, E., Martinez-Manez, R., and Pingarron, J.M. (2013). Enzyme-controlled sensing-actuating nanomachine based on Janus Au-mesoporous silica nanoparticles. Chem. Eur. J. *19*, 7889–7894.

Waki, M., Fujita, S., and Inagaki, S. (2014). Ionic conductivity of mesoporous electrolytes with a high density of pyridinium groups within their framework. J. Mater. Chem. A *2*, 9960–9963.

Wang, J., Pan, M., Yuan, J., Lin, Q., Zhang, X., Liu, G., and Zhu, L. (2020). Hollow mesoporous silica with a hierarchical shell from in situ synergistic soft–hard double templates. Nanoscale *12*, 10863–10871.

Wang, L., Huo, M., Chen, Y., and Shi, J. (2017). Coordination-accelerated "iron extraction" enables fast biodegradation of mesoporous silica-based hollow nanoparticles. Adv. Healthc. Mater *6*, 1700720.

Wang, L., Wang, E., and Tang, J. (2019a). Facile synthesis of flower-like Ag nanocube@mesoporous SiO2 and their sensitive SERS performance. J. Nanopart Res. *21*, 63.

Wang, S., Chen, Z., Zhang, H., Guo, Y., Wang, B., Li, L., Tian, G., Wei, X., Zhu, D., Li, Y., et al. (2013). Synthesis and structural evolution of hollow flower-type mesoporous silica microspheres. J. Mater. Sci. *48*, 2268–2276.

Wang, Y. (2010). Synthesis and formation of hierarchical mesoporous silica network in acidic aqueous solutions of sodium silicate and cationic surfactant. Colloid J. *72*, 737–742.

Wang, Y., Du, X., Liu, Z., Shi, S., and Lv, H. (2019b). Dendritic fibrous nano-particles (DFNPs): rising stars of mesoporous materials. J. Mater. Chem. A *7*, 5111–5152.

Wang, Y., Nor, Y.A., Song, H., Yang, Y., Xu, C., Yu, M., and Yu, C. (2016). Small-sized and large-pore dendritic mesoporous silica nanoparticles enhance antimicrobial enzyme delivery. J. Mater. Chem. B *4*, 2646–2653.

Wang, Y., Zhao, Q., Han, N., Bai, L., Li, J., Liu, J., Che, E., Hu, L., Zhang, Q., Jiang, T., et al. (2015). Mesoporous silica nanoparticles in drug delivery and biomedical applications. Nanomedicine *11*, 313–327.

Wang, Z., Zhang, F., Shao, D., Chang, Z., Wang, L., Hu, H., Zheng, X., Li, X., Chen, F., Tu, Z., et al. (2019c). Janus nanobullets combine photodynamic therapy and magnetic hyperthermia to potentiate synergetic anti-metastatic immunotherapy. Adv. Sci. *6*, 1901690.

Wen, J., Yang, K., Liu, F., Li, H., Xu, Y., and Sun, S. (2017). Diverse gatekeepers for mesoporous silica nanoparticle based drug delivery systems. Chem. Soc. Rev. *46*, 6024–6045.

Williams, D.F. (2008). On the mechanisms of biocompatibility. Biomaterials *29*, 2941–2953.

Wu, M., Chen, W., Chen, Y., Zhang, H., Liu, C., Deng, Z., Sheng, Z., Chen, J., Liu, X., Yan, F., et al. (2018). Focused ultrasound-augmented delivery of biodegradable multifunctional nanoplatforms for imaging-guided brain tumor treatment. Adv. Sci. *5*, 1700474.

Wu, M., Meng, Q., Chen, Y., Du, Y., Zhang, L., Li, Y., Zhang, L., and Shi, J. (2015). Large-pore ultrasmall mesoporous organosilica nanoparticles: micelle/precursor Co-templating assembly and nuclear-targeted gene delivery. Adv. Mater. *27*, 215–222.

Wu, S.-H., Hung, Y., and Mou, C.-Y. (2011). Mesoporous silica nanoparticles as nanocarriers. Chem. Commun. *47*, 9972–9985.

Wu, S.-H., Mou, C.-Y., and Lin, H.-P. (2013). Synthesis of mesoporous silica nanoparticles. Chem. Soc. Rev. *42*, 3862–3875.

Xia, Y. (2008). Nanomaterials at work in biomedical research. Nat. Mater. *7*, 758–760.

Xu, C., Yu, M., Noonan, O., Zhang, J., Song, H., Zhang, H., Lei, C., Niu, Y., Huang, X., Yang, Y., et al. (2015). Core-cone structured monodispersed mesoporous silica nanoparticles with ultra-large cavity for protein delivery. Small *11*, 5949–5955.

Xuan, M., Wu, Z., Shao, J., Dai, L., Si, T., and He, Q. (2016). Near infrared light-powered Janus mesoporous silica nanoparticle motors. J. Am. Chem. Soc. *138*, 6492–6497.

Yamada, H., Urata, C., Aoyama, Y., Osada, S., Yamauchi, Y., and Kuroda, K. (2012). Preparation of colloidal mesoporous silica nanoparticles with different diameters and their unique degradation behavior in static aqueous systems. Chem. Mater. *24*, 1462–1471.

Yanes, R.E., and Tamanoi, F. (2012). Development of mesoporous silica nanomaterials as a vehicle for anticancer drug delivery. Ther. Deliv. *3*, 389–404.

Yang, B., Chen, Y., and Shi, J. (2019). Mesoporous silica/organosilica nanoparticles: synthesis, biological effect and biomedical application. Mater. Sci. Eng. R Rep. *137*, 66–105.

Yang, L., Yin, T., Liu, Y., Sun, J., Zhou, Y., and Liu, J. (2016a). Gold nanoparticle-capped mesoporous silica-based H2O2-responsive controlled release system for Alzheimer's disease treatment. Acta Biomater. *46*, 177–190.

Yang, Y., Lu, Y., Abbaraju, P.L., Zhang, J., Zhang, M., Xiang, G., and Yu, C. (2017). Multi-shelled dendritic mesoporous organosilica hollow spheres: roles of composition and architecture in cancer immunotherapy. Angew. Chem. Int. Ed. *56*, 8446–8450.

Yang, Y., Wan, J., Niu, Y., Gu, Z., Zhang, J., Yu, M., and Yu, C. (2016b). Structure-dependent and glutathione-responsive biodegradable dendritic mesoporous organosilica nanoparticles for safe protein delivery. Chem. Mater. *28*, 9008–9016.

Yonemitsu, M., Tanaka, Y., and Iwamoto, M. (1998). Metal ion-planted MCM-41. J. Catal. *178*, 207–213.

Yu, C., Qian, L., Ge, J., Fu, J., Yuan, P., Yao, S.C.L., and Yao, S.Q. (2016). Cell-penetrating poly (disulfide) assisted intracellular delivery of mesoporous silica nanoparticles for inhibition of miR-21 function and detection of subsequent therapeutic effects. Angew. Chem. Int. Ed. *55*, 9272–9276.

Zhang, H., Xu, H., Wu, M., Zhong, Y., Wang, D., and Jiao, Z. (2015a). A soft–hard template approach towards hollow mesoporous silica nanoparticles with rough surfaces for controlled drug delivery and protein adsorption. J. Mater. Chem. B *3*, 6480–6489.

Zhang, Y., Ang, C.Y., Li, M., Tan, S.Y., Qu, Q., Luo, Z., and Zhao, Y. (2015b). Polymer-coated hollow mesoporous silica nanoparticles for triple-responsive drug delivery. ACS Appl. Mater. Inter. *7*, 18179–18187.

Zhang, L., Zhang, W., Shi, J., Hua, Z., Li, Y., and Yan, J. (2003). A new thioether functionalized organic–inorganic mesoporous composite as a highly selective and capacious Hg2+ adsorbent. Chem. Commun. *9*, 210–211.

Zhao, T., Chen, L., Wang, P., Li, B., Lin, R., Abdulkareem Al-Khalaf, A., Hozzein, W.N., Zhang, F., Li, X., and Zhao, D. (2019). Surface-kinetics mediated mesoporous multipods for enhanced bacterial adhesion and inhibition. Nat. Commun. *10*, 4387.

Zheng, Y., Wang, D., Li, Z., Sun, X., Gao, T., and Zhou, G. (2018). Laccase biosensor fabricated on flower–shaped yolk–shell SiO2 nanospheres for catechol detection. Colloids Surf. A. *538*, 202–209.

Zhou, M., Du, X., Li, W., Li, X., Huang, H., Liao, Q., Shi, B., Zhang, X., and Zhang, M. (2017). One-pot synthesis of redox-triggered biodegradable hybrid nanocapsules with a disulfide-bridged silsesquioxane framework for promising drug delivery. J. Mater. Chem. B *5*, 4455–4469.